4

Engineering Wave Properties

Dedication

SIR GEORGE BIDDELL AIRY

Sir George Biddell Airy (1801–1892) was an astronomer who worked in a variety of areas of science, as did his contemporary and personal acquaintance, Laplace. His major work with respect to this book is his development of small-amplitude water wave theory published in an article in the *Encyclopedia Metropolitan*.

Airy was born in Alnwich, Northumberland, England, and attended Trinity College, Cambridge, from 1819 to 1823. In 1826 he was appointed the Lucasian Chair of Mathematics at Cambridge (once held by Isaac Newton). At that time he worked in optics and drew a great deal of attention to the problem of astigmatism, a vision deficiency from which he suffered.

In 1828 he was named the Plumian Professor of Astronomy and Director of the Cambridge Observatory. He became the Astronomer Royal in 1835, a position he held for 46 years. During that time, he and the observatory staff reduced all measurements made by the observatory between 1750 and 1830.

His research (over 377 papers) encompassed magnetism, tides, geography, gravitation, partial differential equations, and sound. In 1867 his paper on suspension bridges received the Telford Medal of the Institution of Civil Engineers.

His *Numerical Theory of Tides* was published in 1886 despite the presence of several inexplicable errors. He attempted (unsuccessfully) to resolve these until 1888. He died in 1892.

4.1 INTRODUCTION

The solutions developed in Chapter 3 for standing and progressive small-amplitude water waves provide the basis for applications to numerous problems of engineering interest. For example, the water particle kinematics and the pressure field within the waves are directly related to the calculation of forces on bodies. The transformation of waves as they propagate toward shore is also important, as in many cases coastal engineering design involves the forecasting of offshore wave climates or the use of offshore data, for example, those obtained from ships. It is obviously necessary to be able to determine any modifications that occur to these waves as they encounter shallower water and approach the shore.

4.2 WATER PARTICLE KINEMATICS FOR PROGRESSIVE WAVES

Consider a progressive wave with water surface displacement given by

$$\eta = \frac{H}{2} \cos (kx - \sigma t)$$

The associated velocity potential is

$$\phi = -\frac{H}{2} \frac{g}{\sigma} \frac{\cosh k(h + z)}{\cosh kh} \sin (kx - \sigma t) \tag{4.1}$$

By introducing the dispersion relationship, $\sigma^2 = gk \tanh kh$, this can be written as

$$\phi = -\frac{H}{2} C \frac{\cosh k(h + z)}{\sinh kh} \sin (kx - \sigma t) \tag{4.2}$$

4.2.1 Particle Velocity Components

The horizontal velocity under the wave is given by definition, Eq. (2.68), as

$$u = -\frac{\partial \phi}{\partial x} = \frac{H}{2} \sigma \frac{\cosh k(h + z)}{\sinh kh} \cos (kx - \sigma t) \tag{4.3a}$$

or

$$u = \frac{gHk}{2\sigma} \frac{\cosh k(h + z)}{\cosh kh} \cos (kx - \sigma t) \tag{4.3b}$$

The local horizontal acceleration is then

$$\frac{\partial u}{\partial t} = \frac{H}{2}\sigma^2 \frac{\cosh k(h+z)}{\sinh kh} \sin(kx - \sigma t) \tag{4.4}$$

and the vertical velocity and local acceleration are

$$w = -\frac{\partial \phi}{\partial z} = \frac{H}{2}\sigma \frac{\sinh k(h+z)}{\sinh kh} \sin(kx - \sigma t) \tag{4.5}$$

$$\frac{\partial w}{\partial t} = -\frac{H}{2}\sigma^2 \frac{\sinh k(h+z)}{\sinh kh} \cos(kx - \sigma t) \tag{4.6}$$

Examining the horizontal and vertical velocity components as a function of position, it is clear that they are 90° out of phase; the extreme values of the horizontal velocity appear at the phase positions $(kx - \sigma t) = 0, \pi, \ldots$ (under the crest and trough positions), while the extreme vertical velocities appear at $\pi/2, 3\pi/2, \ldots$ (where the water surface displacement is zero).

The vertical variation of the velocity components is best viewed by starting at the bottom where $k(h + z) = 0$. Here the hyperbolic terms involving z in both the u and w velocities are at their minima, 1 and 0, respectively. As we progress upward in the fluid, the magnitudes of the velocity components increase. In Figure 4.1, the velocity components are plotted for four phase positions. The accelerations are such that the maximum vertical accelerations occur as the horizontal velocities are extremes and the same is true for the vertical velocities and the horizontal accelerations.

4.2.2 Particle Displacements

A water particle with a mean position of, say, (x_1, z_1) will be displaced by the wave-induced pressures and the instantaneous water particle position will be denoted as $(x_1 + \zeta, z_1 + \xi)$, as shown in Figure 4.2. The displacement components (ζ, ξ) of the water particle can be found by integrating the velocity with respect to time.

$$\zeta(x_1, z_1, t) = \int u(x_1 + \zeta, z_1 + \xi)\, dt \tag{4.7}$$

$$\xi(x_1, z_1, t) = \int w(x_1 + \zeta, z_1 + \xi)\, dt \tag{4.8}$$

In keeping with our small-amplitude wave considerations, ζ and ξ will be small quantities and therefore we can replace $u(x_1 + \zeta, z_1 + \xi)$ with $u(x_1, z_1)$.[1]

[1]This involves neglecting terms such as $\frac{\partial u}{\partial x}\zeta$, as can be seen from a Taylor series expansion.

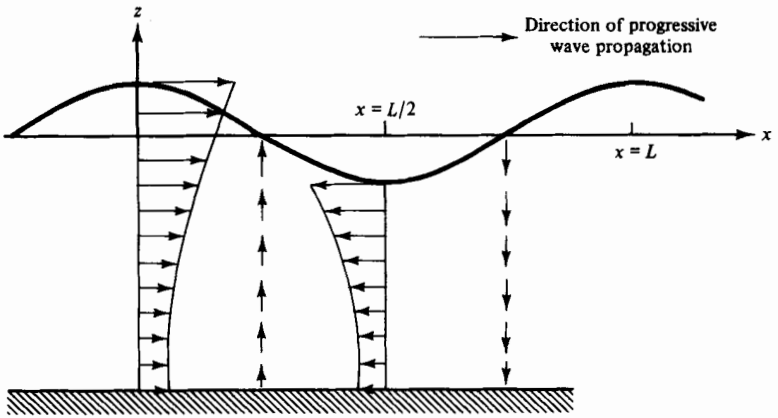

Figure 4.1 Water particle velocities in a progressive wave.

Integrating the equations above then yields

$$\zeta = -\frac{H}{2}\frac{gk}{\sigma^2}\frac{\cosh k(h+z_1)}{\cosh kh}\sin(kx_1 - \sigma t) \tag{4.9}$$

or

$$\zeta = -\frac{H}{2}\frac{\cosh k(h+z_1)}{\sinh kh}\sin(kx_1 - \sigma t)$$

using the dispersion relationship. The vertical displacement is determined similarly:

$$\xi = \frac{H}{2}\frac{\sinh k(h+z_1)}{\sinh kh}\cos(kx_1 - \sigma t) \tag{4.10}$$

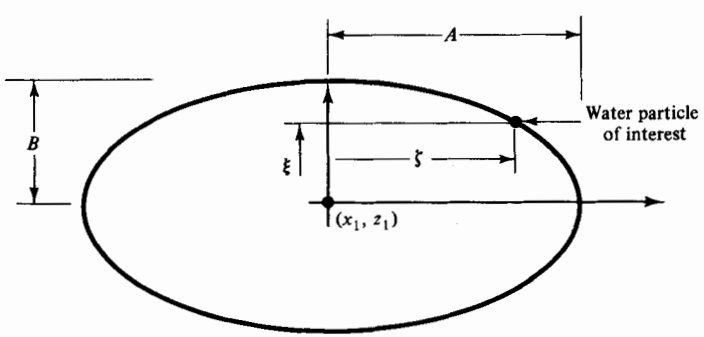

Figure 4.2 Elliptical form of water particle trajectory.

The displacements ζ and ξ can be rewritten as

$$\zeta(x_1, z_1, t) = -A \sin(kx_1 - \sigma t) \tag{4.11}$$

$$\xi(x_1, z_1, t) = B \cos(kx_1 - \sigma t) \tag{4.12}$$

Squaring and adding yields the water particle trajectory as

$$\left(\frac{\zeta}{A}\right)^2 + \left(\frac{\xi}{B}\right)^2 = 1 \tag{4.13}$$

which is the equation of an ellipse with semiaxes A and B in the x-z direction, respectively (Figure 4.2). We should note also that A is always greater than or equal to B. In fact, at the locations of the mean water level, the water particles with mean elevation $z = 0$, follow a closed trajectory with vertical displacement $H/2$; that is, these particles comprise the surface. There are no water particles with mean locations higher than $z = 0$.

In *shallow water* ($h/L < 1/20$), using the shallow water approximations, the major semiaxis reduces to

$$A = \frac{H}{2}\frac{\cosh k(h + z_1)}{\sinh kh} = \frac{H}{2}\frac{1}{kh} = \frac{HL}{4\pi h} = \frac{HT}{4\pi}\sqrt{\frac{g}{h}} \tag{4.14}$$

where the equality for shallow water, $L = CT = \sqrt{gh}\,T$, has been introduced. The minor semiaxis B can be determined similarly.

$$B = \frac{H}{2}\frac{\sinh k(h + z_1)}{\sinh kh} = \frac{H}{2}\left(1 + \frac{z_1}{h}\right) \tag{4.15}$$

Note that A is not a function of elevation. The horizontal excursion of a water particle is a constant distance for all particles under the wave. The total vertical excursion increases linearly with elevation, being zero, of course, at the bottom and being H at the mean water surface, $z = 0$.

For *deep water* waves ($h/L \geqslant \frac{1}{2}$) it can be shown that the semiaxes simplify to

$$A = \frac{H}{2}\frac{e^{kh}e^{kz_1}}{e^{kh}} = \frac{H}{2}e^{kz_1} \tag{4.16}$$

$$B = \frac{H}{2}e^{kz_1} = A \tag{4.17}$$

The trajectories are circles which decay exponentially with depth. For a depth of $z = -L/2$, the values of A and B have been reduced by the amount $e^{-\pi}$, or the radii of the circles are only 4% of the surface values, essentially negligible. Figure 4.3 displays the shapes of the water particle trajectories for different relative depths.

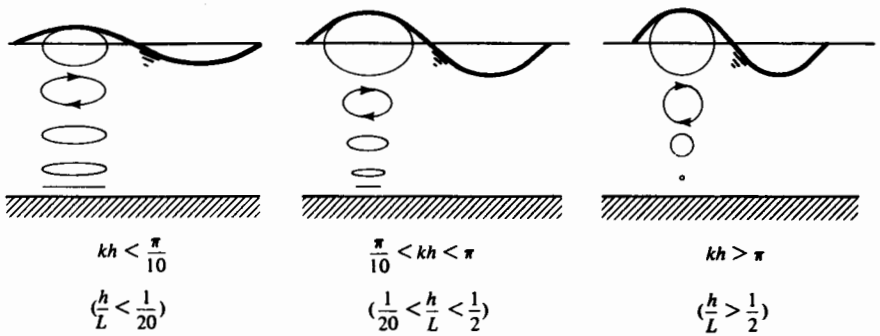

Figure 4.3 Water particle trajectories in progressive water waves of different relative depths.

4.3 PRESSURE FIELD UNDER A PROGRESSIVE WAVE

The pressure field associated with a progressive wave is determined from the unsteady Bernoulli equation developed for an ideal fluid and the velocity potential appropriate to this case, Eq. (2.92):

$$\frac{p}{\rho} + gz + \tfrac{1}{2}(u^2 + w^2) - \frac{\partial \phi}{\partial t} = C(t) \tag{4.18}$$

Equating the relationship above at any depth z, and at the free surface η, where the pressure is taken as zero, and linearizing yields

$$\left(\frac{p}{\rho} + gz - \frac{\partial \phi}{\partial t}\right)_z = g\eta - \left.\frac{\partial \phi}{\partial t}\right|_{\eta \approx 0} \tag{4.19}$$

Recalling from Chapter 3 that the linearized DFSBC reduces to

$$\eta = \left.\frac{1}{g}\frac{\partial \phi}{\partial t}\right|_{z=0} \tag{4.20}$$

it is seen that the pressure can be expressed as

$$\frac{p}{\rho} = -gz + \frac{\partial \phi}{\partial t} \tag{4.21}$$

where the small velocity squared terms have been neglected.

For a progressive wave described by the velocity potential in Eq. (4.1), we have

$$p = -\rho g z + \rho g \frac{H}{2} \frac{\cosh k(h+z)}{\cosh kh} \cos(kx - \sigma t) \tag{4.22}$$

or

$$p = -\rho g z + \rho g \eta K_p(z) \tag{4.23}$$

where

$$K_p(z) = \frac{\cosh k(h+z)}{\cosh kh} \tag{4.24}$$

The first term on the right-hand side of the pressure equation (4.23) is, of course, the hydrostatic term, which would exist without the presence of the waves. The second term is called the dynamic pressure. The term $K_p(z)$ is referred to as the "pressure response factor" and below the mean water surface is always less than unity.

The dynamic pressure is a result of two contributions; the first and most obvious contributor is the surcharge of pressure due to the presence of the free surface displacement. If the pressure response factor were unity, the pressure contribution from the free surface displacement would be purely hydrostatic. However, associated with the wave motion is the vertical acceleration, which is 180° out of phase with the free surface displacement. This contribution modifies the pressure from the purely hydrostatic case. The reader may wish to verify that Eq. (4.22) can be obtained by integrating the linearized vertical equation of motion, Eq. (2.38c), from any depth z up to the free surface η. In Figure 4.4, the effect of the dynamic pressure in modifying the hydrostatic pressure is shown.

The pressure response factor has a maximum of unity at $z = 0$, and a minimum of 1/cosh kh at the bottom. To determine the pressure above the mean water level we again must use the Taylor series for a small positive distance z_1 $(0 < z_1 < \eta)$:

$$p(z_1) = (-\rho gz + \rho g\eta K_p)_{z=0} + z_1 \frac{\partial}{\partial z}(-\rho gz + \rho g\eta K_p)_{z=0} + \cdots \tag{4.25}$$

$$= \rho g\eta - \rho gz_1 \qquad \text{to the first order}$$

$$= \rho g(\eta - z_1) \tag{4.26}$$

Thus to this approximation the pressure is hydrostatic under the wave crest

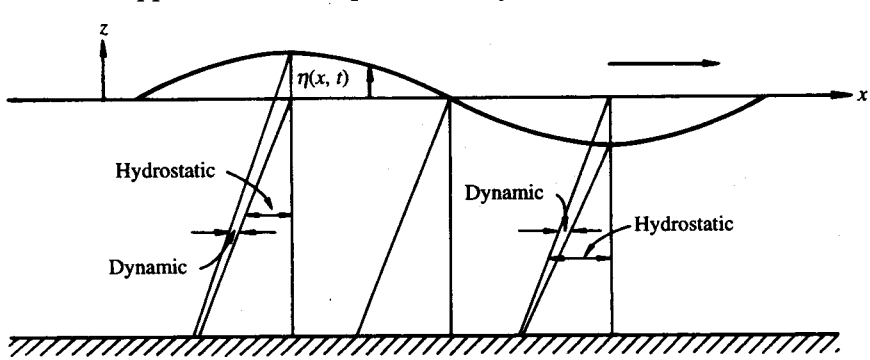

Figure 4.4 Hydrostatic and dynamic pressure components at various phase positions in a progressive water wave.

down to $z = 0$. Below that depth, however, it deviates from the hydrostatic law. Note also that Eq. (4.26) predicts a zero pressure at the instantaneous free surface, $z_1 = \eta$. Figure 4.5 shows the isolines of pressure under a wave for $h/L = 0.2$.

One method of measuring waves in either the laboratory or field is by sensing the pressure fluctuations and then calculating the associated water surface displacements by Eq. (4.23). From Eq. (4.23), a bottom-mounted pressure gage would record a steady hydrostatic pressure plus the oscillating dynamic pressure, which for a particular wave period is proportional to the free surface displacement η, the variable of interest. If the dynamic pressure p_D is isolated by subtracting out the mean hydrostatic pressure, then η is

$$\eta = \frac{p_D}{\rho g K_p(-h)} \quad \text{and} \quad K_p(-h) = \frac{1}{\cosh kh} \tag{4.27}$$

where $K_p(-h)$ is a function of the angular frequency of the waves. Thus the dispersion relationship must be used to determine kh from the frequency of the observed waves. If a mean current is present, the wave number must be computed via Eq. (3.52); otherwise, significant errors can occur.

Even though we have derived the pressure response factor for only one frequency component, it is interesting to note that for cases in which the linear assumption is reasonably valid, Eq. (4.27) can be used to determine the composite wave system containing many (or an infinite) number of components from a measured pressure time series.

Because of the dependency of the pressure response factor on the wave frequency, short-period waves have a very small K_p (at the bottom), while for long-period waves K_p approaches unity. In other words, very short period waves may not even be recorded by the pressure gage. The reader may wish to

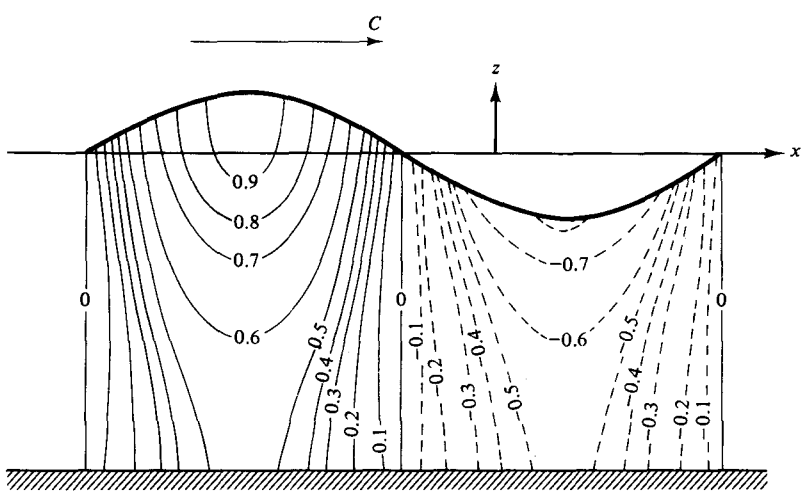

Figure 4.5 Isolines of $p_D/[\gamma(H/2)]$ for progressive wave of $h/L = 0.20$.

show that the shallow and deep water asymptotes for the pressure response factor are unity and e^{kz}, respectively.

4.4 WATER PARTICLE KINEMATICS FOR STANDING WAVES

The original velocity potential we derived represented a pure standing wave,

$$\phi = \frac{H_s g}{2\sigma} \frac{\cosh k(h+z)}{\cosh kh} \cos kx \sin \sigma t \tag{4.28}$$

with

$$\eta = \frac{H_s}{2} \cos kx \cos \sigma t \tag{4.29}$$

$$\sigma^2 = gk \tanh kh \tag{4.30}$$

where H_s denotes the height of the standing wave and is twice the height of each of the two progressive waves forming the standing wave.

The velocity potential for a standing wave can be rederived by subtracting the velocity potential for two progressive waves of the same period with heights H_p propagating in opposite directions.

$$\phi = -\frac{H_p}{2}\frac{g}{\sigma}\frac{\cosh k(h+z)}{\cosh kh} \sin (kx - \sigma t) + \frac{H_p}{2}\frac{g}{\sigma}\frac{\cosh k(h+z)}{\cosh kh} \sin (kx + \sigma t) \tag{4.31}$$

Sin $(kx \pm \sigma t)$ can be rewritten as sin kx cos $\sigma t \pm$ cos kx sin σt, (from trigonometry) and thus the velocity potential is rewritten as

$$\phi = \frac{H_p g}{\sigma} \frac{\cosh k(h+z)}{\cosh kh} \cos kx \sin \sigma t \tag{4.32}$$

Comparing the two velocity potentials, it is clear that $H_p = H_s/2$. Therefore, a standing wave of height H_s is composed of two progressive waves propagating in opposite directions, each with height equal to one-half that of the standing wave.

4.4.1 Velocity Components

The velocities under a standing wave are readily found to be

$$u = -\frac{\partial \phi}{\partial x} = \frac{H}{2}\frac{gk}{\sigma}\frac{\cosh k(h+z)}{\cosh kh} \sin kx \sin \sigma t \tag{4.33}$$

$$w = -\frac{\partial \phi}{\partial z} = -\frac{H}{2}\frac{gk}{\sigma}\frac{\sinh k(h+z)}{\cosh kh} \cos kx \sin \sigma t \tag{4.34}$$

where for convenience the subscript s has been dropped. Using the dispersion relationship,

$$u = \frac{H}{2}\sigma\frac{\cosh k(h+z)}{\sinh kh}\sin kx \sin \sigma t \tag{4.35a}$$

$$w = -\frac{H}{2}\sigma\frac{\sinh k(h+z)}{\sinh kh}\cos kx \sin \sigma t \tag{4.35b}$$

As with the velocities under a progressive wave, these velocities increase with elevation above the bottom. The extreme values of u and w in space occur under the nodes and antinodes of the water surface profile as shown in Figure 4.6, where u and w are zero under the antinodes and nodes, respectively. It is of interest that the horizontal and vertical components of velocity under a standing wave are in phase; that is, the time-varying term "sin σt" modifies both velocity components and, at certain times, the velocity is zero everywhere in the standing wave system. It is therefore evident that at some times all the energy is potential and, by reference to Eqs. (4.35), at other times all the energy is kinetic.

If a progressive wave were normally incident on a vertical wall, it would be reflected backward without a change in height, thus giving a standing wave in front of the wall. The lateral boundary condition at the vertical wall would be one of no flow through the wall, or $u = -\partial\phi/\partial x = 0$ at $x = x_{\text{wall}}$, where x_{wall} is the location of the wall. Inspection of the equation for the horizontal velocity, Eq. (4.33), shows that at locations $kx = n\pi$ (where n is an integer), the no-flow boundary condition is satisfied. Therefore, a standing wave could exist within a basin with two walls situated at two antinodes of a standing wave. This is, in fact, the simplest model of uniform depth lakes, estuaries, and harbors where standing waves, called seiches, can be generated by winds, earthquakes, or other phenomena. We examine these waves further in Chapter 5.

The local accelerations under a standing wave are

$$\frac{\partial u}{\partial t} = \frac{H}{2}\sigma^2\frac{\cosh k(h+z)}{\sinh kh}\sin kx \cos \sigma t \tag{4.36}$$

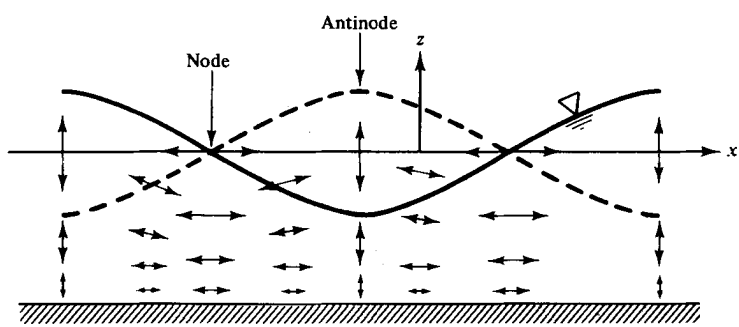

Figure 4.6 Distribution of water particle velocities in a standing water wave.

$$\frac{\partial w}{\partial t} = -\frac{H}{2}\sigma^2 \frac{\sinh k(h+z)}{\sinh kh} \cos kx \cos \sigma t \tag{4.37}$$

Under the wave antinodes, the vertical accelerations are maxima, while the horizontal accelerations are zero, and under the nodes, the opposite is true.

4.4.2 Particle Displacements

The displacements of a water particle (ζ, ξ) from its mean position (x_1, z_1) under a standing wave are defined in a linearized fashion as before.

$$\zeta = \int u(x_1 + \zeta, z_1 + \xi)\, dt \approx \int u(x_1, z_1)\, dt \tag{4.38}$$

$$\xi = \int w(x_1 + \zeta, z_1 + \xi)\, dt \approx \int w(x_1, z_1)\, dt \tag{4.39}$$

or

$$\zeta = -\frac{H}{2}\frac{\cosh k(h+z_1)}{\sinh kh} \sin kx_1 \cos \sigma t = -A \cos \sigma t \tag{4.40}$$

$$\xi = \frac{H}{2}\frac{\sinh k(h+z_1)}{\sinh kh} \cos kx_1 \cos \sigma t = B \cos \sigma t \tag{4.41}$$

The displacement vector is $\mathbf{r} = \zeta\mathbf{i} + \xi\mathbf{k}$; its magnitude $|\mathbf{r}|$ is

$$|\mathbf{r}| = \sqrt{A^2 + B^2} \cos \sigma t \tag{4.42}$$

or

$$|\mathbf{r}(t)| = \frac{H}{2}\frac{\cos \sigma t}{\sinh kh} \sqrt{\cosh^2 k(h+z_1) \sin^2 kx_1 + \sinh^2 k(h+z_1) \cos^2 kx_1} \tag{4.43}$$

For infinitesimally small motions, the displacement vector is a straight line,[2] the amplitude and inclination being dependent on position (x_1, z_1). The water particle under the standing wave moves back and forth along the line with time. Substituting the trigonometric identities,

$$\cosh^2 k(h+z_1) = \tfrac{1}{2}[\cosh 2k(h+z_1) + 1]$$

$$\sin^2 kx_1 = \tfrac{1}{2}(1 - \cos 2kx_1)$$

$$\sinh^2 k(h+z_1) = \tfrac{1}{2}[\cosh 2k(h+z_1) - 1]$$

$$\cos^2 kx_1 = \tfrac{1}{2}(1 + \cos 2kx_1)$$

yields from Eq. (4.43),

$$|\mathbf{r}(t)| = \frac{H \cos \sigma t}{4 \sinh kh} \sqrt{2[\cosh 2k(h+z_1) - \cos 2kx_1]}$$

[2]From Equations (4.40) and (4.41), we obtain $\xi = -(B/A)\zeta$ which may be compared with Eq. (4.13), the equation for the trajectories of a progressive wave.

Note that at the bottom under the antinodes $|\mathbf{r}|$ is zero. The maximum value of $|\mathbf{r}|$ occurs under the nodes, where $\cos 2kx_1 = -1$.

The motion of the water particles under a standing wave can thus be described as a simple harmonic motion along a straight line. The slope of the displacement vector θ is given by

$$\tan\theta = \frac{\xi}{\zeta} = -\frac{\tanh k(h+z_1)}{\tan kx_1} \tag{4.44}$$

which is not a function of time. Clearly, at the bottom, the trajectories are horizontal ($\theta = 0$), as is to be expected by the bottom boundary condition. Figure 4.6 portrays the water particle trajectories at several phase positions under a standing wave.

4.5 PRESSURE FIELD UNDER A STANDING WAVE

To find the pressure at any depth under a standing wave, the unsteady Bernoulli equation is used as in the case for progressive waves.

$$\frac{p}{\rho} + \frac{u^2 + w^2}{2} - \frac{\partial\phi}{\partial t} + gz = C(t) \tag{4.45}$$

Linearizing and evaluating as before between the free surface and at some depth (z) in the fluid, the gage pressure is

$$p = -\rho gz + \rho\frac{\partial\phi}{\partial t}$$

or

$$p = -\rho gz + \rho g\frac{H\cosh k(h+z)}{2\cosh kh}\cos kx\cos\sigma t$$

$$= -\rho gz + \rho g K_p(z)\eta \tag{4.46}$$

where the pressure response factor $K_p(z)$ is the same as determined for progressive waves. Note that under the nodes, the pressure is solely hydrostatic. Again, the dynamic pressure is in phase with the water surface elevation, and as before it is a combined result of the local water surface displacement and the vertical accelerations of the overlying water particles.

The force exerted on a wall at an antinode can be calculated by integrating the pressure over depth per unit width of wall

$$F = \int_{-h}^{\eta_w} p(z)\,dz = \int_{-h}^{0}\left[-\rho gz + \rho g\eta_w\frac{\cosh k(h+z)}{\cosh kh}\right]dz + \int_{0}^{\eta_w}\rho g(\eta_w - z)\,dz$$

from Eqs. (4.26) and (4.46) and where $\eta_w = (H/2)\cos\sigma t$, the water surface

displacement at the wall. It should be stressed that this formulation is not entirely consistent, as the second integral on the right-hand side representing the force contribution of the wave crest region is of second order; yet second-order terms in the form of the square of the velocity components have already been dropped from the first term of the right-hand side. Integrating, we get

$$F = \rho g\left(\frac{h^2 + \eta_w^2}{2}\right) + \rho g h \frac{\tanh kh}{kh} \eta_w \tag{4.47}$$

To first order,

$$F = \rho \frac{gh^2}{2} + \rho g h \frac{\tanh kh}{kh} \eta_w \tag{4.48}$$

The force on the wall consists of the hydrostatic contribution, plus an oscillatory term due to the dynamic pressure. The maximum force occurs when $\eta_w = H/2$,

$$F_{\max} = \rho g \frac{(4h^2 + (H)^2)}{8} + \rho g h \frac{H}{2} \frac{\tanh kh}{kh} \tag{4.49}$$

4.6 PARTIAL STANDING WAVES

For the case just considered of pure standing waves, two waves of the same period and height, but propagating in opposite directions, were superimposed, as one expects from the perfect reflection of an incident wave from a vertical wall. Quite often in nature, however, when waves are reflected from obstacles, not all of the wave energy is reflected; some is absorbed by the obstacle and some is transmitted past the obstacle. For example, waves are reflected from breakwaters and beaches; in each case wave energy is not perfectly reflected. To examine this case, let us assume that the incident wave has a height H_i, but that the reflected wave has a smaller height H_r and different phase than the incident wave. The wave periods of the incident and reflected waves will be the same. The total wave profile seaward of the obstacle is then

$$\eta_t = \frac{H_i}{2} \cos(kx - \sigma t) + \frac{H_r}{2} \cos(kx + \sigma t + \epsilon) \tag{4.50a}$$

where ϵ is the phase lag induced by the reflection process. If the water surface displacements are plotted, they appear as in Figure 4.7. Due to the imperfect reflection, there are no true nodes in the wave profile.

Quite often in measuring wave heights in a wave tank, reflections occur and it is necessary to be able to separate out the incident and reflected wave

heights. To do this, we rewrite η_t, using trigonometric identities.

$$\eta_t = \frac{H_i}{2}(\cos kx \cos \sigma t + \sin kx \sin \sigma t) + \frac{H_r}{2}(\cos (kx + \epsilon) \cos \sigma t - \sin (kx + \epsilon) \sin \sigma t)$$

Grouping similar time terms,

$$\eta_t = \left[\frac{H_i}{2} \cos kx + \frac{H_r}{2} \cos (kx + \epsilon)\right] \cos \sigma t + \left[\frac{H_i}{2} \sin kx - \frac{H_r}{2} \sin (kx + \epsilon)\right] \sin \sigma t$$

or, for convenience, denoting the bracketed terms by $I(x)$ and $F(x)$,

$$\eta_t = I(x) \cos \sigma t + F(x) \sin \sigma t \tag{4.50b}$$

Thus η_t is a sum of standing waves. To find the extreme values of η_t for any x, that is, the envelope of the wave heights, denoted by the dotted lines in the figure, it is necessary to find the maximas and minimas of η_t with respect to time. Proceeding as usual by taking the first derivative and setting it equal to zero to find the extremes yields

$$\frac{\partial \eta_t}{\partial t} = -I(x)\sigma \sin \sigma t + F(x)\sigma \cos \sigma t = 0 \tag{4.51}$$

or

$$\tan (\sigma t)_m = \frac{F(x)}{I(x)}$$

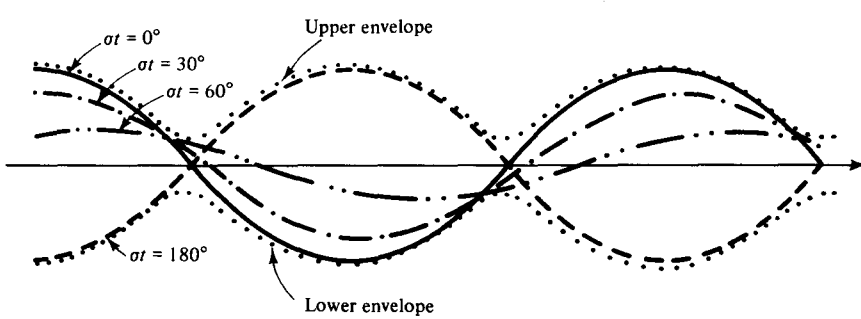

Figure 4.7 Instantaneous water surface displacements and envelope in a partial standing wave system.

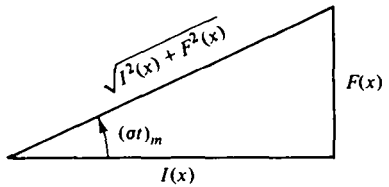

Figure 4.8 Relationships among $(\sigma t)_m$, $F(x)$, and $I(x)$.

Therefore, to find the maxima and minima of η_t, $(\sigma t)_m$ is substituted into Eq. (4.50a). Examining Figure 4.8, it is clear that

$$\cos(\sigma t)_m = \frac{I(x)}{\sqrt{I^2(x) + F^2(x)}}$$

$$\sin(\sigma t)_m = \frac{F(x)}{\sqrt{I^2(x) + F^2(x)}}$$

Substituting into Equation (4.50b),[3] we have

$$(\eta_t)_m = \frac{I^2(x) + F^2(x)}{\sqrt{I^2(x) + F^2(x)}} = \pm\sqrt{I^2(x) + F^2(x)} \tag{4.52}$$

Substituting for $I(x)$ and $F(x)$ from Eq. (4.50b), it is seen readily that the extreme values of η_t for any location x are

$$[\eta_t(x)]_m = \pm\sqrt{\left(\frac{H_i}{2}\right)^2 + \left(\frac{H_r}{2}\right)^2 + \frac{H_i H_r}{2}\cos(2kx + \epsilon)} \tag{4.53}$$

$[\eta_t(x)]_m$ obviously varies periodically with x. At the phase positions $(2kx_1 + \epsilon) = 2n\pi$ $(n = 0, 1, \ldots)$, $[\eta_t(x)]_m$ becomes a maximum of the envelope

$$(\eta_t)_{\max} = \tfrac{1}{2}(H_i + H_r), \qquad \text{the quasi-antinodes} \tag{4.54}$$

whereas at the phase positions, $(2kx_2 + \epsilon) = (2n + 1)\pi$ $(n = 0, 1, \ldots)$, the value of $[\eta_t(x)]_m$ becomes a minimum of the envelope:

$$(\eta_t)_{\min} = \tfrac{1}{2}(H_i - H_r), \qquad \text{the quasi-nodes} \tag{4.55}$$

The distance between the quasi-antinode and node can be found by subtracting the phases

$$(2kx_2 + \epsilon) - (2kx_1 + \epsilon) = (2n + 1)\pi - 2n\pi$$

or

$$2k(x_2 - x_1) = \pi$$

$$x_2 - x_1 = \frac{L}{4}$$

[3]This exercise shows simply that the maximum and minimum of $(A \sin \sigma t + B \cos \sigma t)$ are $\pm\sqrt{A^2 + B^2}$.

For a laboratory experiment, where reflection from a beach or an obstacle is present, if the amplitude of the quasi-antinodes and nodes are measured by slowly moving a wave gage along the wave tank, the incident and reflected wave heights are found simply from Eqs. (4.54) and (4.55) as

$$H_i = (\eta_t)_{\max} + (\eta_t)_{\min} \tag{4.56}$$

$$H_r = (\eta_t)_{\max} - (\eta_t)_{\min} \tag{4.57}$$

The reflection coefficient of the obstacle is defined as

$$\kappa_r = \frac{H_r}{H_i} \tag{4.58}$$

Figure 4.9 presents such data for the case of extremely small waves and nearly perfect reflection. To find the phase ϵ, it is necessary to find the distance from origin to the nearest maximum or minimum x_1, and to solve one of the following equations:

$$2kx_1 + \epsilon = \begin{cases} 2n\pi, & n = 0, 1, 2, \ldots \quad \text{for the maximum} \\ (2n+1)\pi, & n = 0, 1, 2, \ldots \quad \text{for the minimum} \end{cases}$$

The reader should verify that the dynamic and hydrostatic pressure under a partial standing wave system can be expressed as

$$p(x, z, t) = -\rho g z + \rho g K_p(z)\eta$$

where $\eta(x, t)$ and $K_p(z)$ are given by Eqs. (4.50a) and (4.24), respectively.

4.7 ENERGY AND ENERGY PROPAGATION IN PROGRESSIVE WAVES

The total energy contained in a wave consists of two kinds: the potential energy, resulting from the displacement of the free surface and the kinetic energy, due to the fact that the water particles throughout the fluid are moving. This total energy and its transmission are of importance in determining how waves change in propagating toward shore, the power required to generate waves, and the available power for wave energy extraction devices, for example.

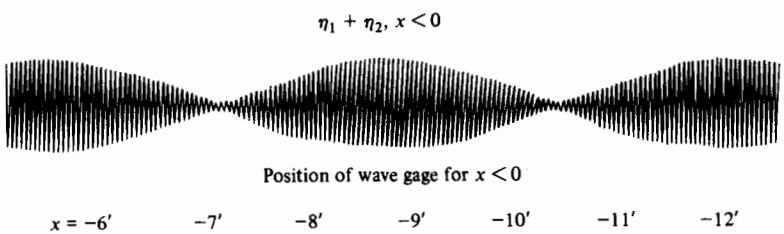

Figure 4.9 Water surface displacement as measured from a slowly moving carriage for the case of nearly perfect reflection. (From Dean and Ursell, 1959.)

4.7.1 Potential Energy

Potential energy as it occurs in water waves is the result of displacing a mass from a position of equilibrium against a gravitational field. When water is at rest with a uniform free surface elevation, it can be shown readily that the potential energy is a minimum. However, a displacement of an assemblage of particles resulting in the displacement of the free surface will require that work be done on the system and results in an increase in potential energy.

We will derive the potential energy associated with a sinusoidal wave by two different methods. First consider the wave shown in Figure 4.10; we will determine the average potential energy per unit surface area associated with the wave as the difference between the potential energy with and without the wave present. The potential energy of a small column of fluid shown in Figure 4.10 with mass dm relative to the bottom is

$$d(\text{PE}) = dmg\bar{z} \tag{4.59}$$

in which $\bar{z}$ is the height to the center of gravity of the mass, and can be written as

$$\bar{z} = \frac{h + \eta}{2} \tag{4.60}$$

and the differential mass per unit width is

$$dm = \rho\,(h + \eta)\,dx$$

The potential energy averaged over one wave length for a progressive wave of height H is then

$$(\overline{\text{PE}})_T \equiv \frac{1}{L}\int_x^{x+L} d(\text{PE}) = \frac{1}{L}\int_x^{x+L} \rho g \frac{(h+\eta)^2}{2}\,dx \tag{4.61}$$

$$= \frac{\rho g}{L}\int_x^{x+L}\left[\frac{1}{2}(h^2 + 2\eta h + \eta^2)\right]dx \tag{4.62}$$

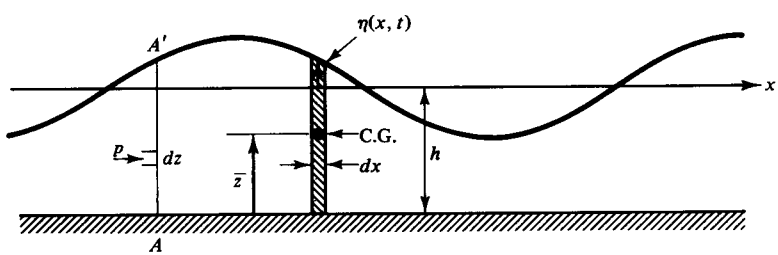

Figure 4.10 Definition sketch for determination of potential energy.

The subscript T signifies that the potential energy of the total water volume is being considered. For $\eta = (H/2)\cos(kx - \sigma t)$, the average potential energy is

$$(\overline{\mathrm{PE}})_T = \frac{\rho g}{L}\left(\frac{1}{2}h^2 L + h\int_x^{x+L}\eta\,dx + \frac{1}{2}\int_x^{x+L}\eta^2\,dx\right) \tag{4.63}$$

The integration is straightforward. For the last integral, we recognize that the sum of the squares of the sine and cosine functions is identically equal to unity, and it can be seen readily that the average of the square of each function over an integral number of one-half wave lengths is one-half. Since this integration is used often in water wave mechanics, the reader should verify this result. The potential energy is now

$$(\overline{\mathrm{PE}})_T = \rho g\frac{h^2}{2} + \rho g\frac{H^2}{16} \tag{4.64}$$

The potential energy due to the waves is the difference between the potential energy with waves present and with no waves present, that is,

$$(\overline{\mathrm{PE}})_{\mathrm{waves}} = (\overline{\mathrm{PE}})_T - (\overline{\mathrm{PE}})_{\mathrm{w/o}} \tag{4.65}$$

or

$$\overline{\mathrm{PE}} \equiv (\overline{\mathrm{PE}})_{\mathrm{waves}} = \frac{\rho g H^2}{16} \tag{4.66}$$

The potential energy of the waves per unit area depends solely on the wave height. Also, although the development was presented for progressive waves, examination of the details of the derivation will show that the results are equally applicable to the case of standing waves which are sinusoidal in form.

Anticipating the application of this result to more realistic cases, we represent the sea surface η_T by a number N of components, each given by

$$\eta_n = \frac{H_n}{2}\cos(k_n x - \sigma_n t - \epsilon_n) \tag{4.67}$$

and

$$\eta_T = \sum_{n=1}^{\infty}\eta_n \tag{4.68}$$

Although it is beyond the scope of the presentation here, the total average potential energy in this case is

$$\overline{\mathrm{PE}} = \frac{\rho g}{16}\sum_{n=1}^{N}H_n^2 \tag{4.69}$$

To return to the case of potential energy due to a sinusoid, it may be worthwhile for the reader to derive the results by a different approach by simply calculating the increase in potential energy required to elevate the

water formerly in the trough to the crest location through a vertical distance $2 \cdot z_{cg}$, where z_{cg} is shown in Figure 4.11. Note that this area is $HL/2\pi$ and the vertical distance from the mean waterline to the centers of gravity is $\pi H/16$.

4.7.2 Kinetic Energy

The kinetic energy is due to the moving water particles; the kinetic energy associated with a small parcel of fluid with mass dm is

$$d(\mathrm{KE}) = dm \frac{u^2 + w^2}{2} = \rho \, dx \, dz \frac{u^2 + w^2}{2} \tag{4.70}$$

To find the average kinetic energy per unit surface area, $d(\mathrm{KE})$ must be integrated over depth and averaged over a wave length.

$$\overline{\mathrm{KE}} = \frac{1}{L} \int_x^{x+L} \int_{-h}^{\eta} \rho \frac{u^2 + w^2}{2} \, dz \, dx \tag{4.71}$$

From the known solution for the velocities under a progressive wave, Eqs. (4.3a) and (4.5), the integral can be written as

$$\overline{\mathrm{KE}} = \frac{\rho}{2L} \left(\frac{gHk}{2\sigma} \frac{1}{\cosh kh} \right)^2 \int_x^{x+L} \int_{-h}^{\eta} [\cosh^2 k(h+z) \cos^2 (kx - \sigma t) + \sinh^2 k(h+z) \sin^2 (kx - \sigma t)] \, dz \, dx \tag{4.72}$$

Using trigonometric identities (just as was done for the trajectories under a

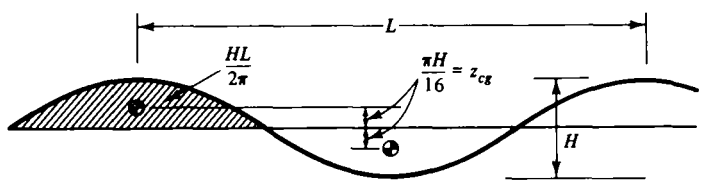

Figure 4.11 Potential energy determined as the result of raising water mass in trough area to crest area.

standing wave), this can be recast as

$$\overline{\mathrm{KE}} = \frac{\rho}{2L}\left(\frac{gHk}{2\sigma}\frac{1}{\cosh kh}\right)^2 \int_x^{x+L}\int_{-h}^{\eta\approx 0}\frac{1}{2}\left[\cosh 2k(h+z) + \cos 2(kx-\sigma t)\right] dz\, dx \tag{4.73}$$

Carrying out the integration and simplifying yields

$$\overline{\mathrm{KE}} = \tfrac{1}{16}\rho g H^2 \tag{4.74}$$

This is equal to the magnitude of the potential energy, which is characteristic of conservative (nondissipative) systems in general. The *total* average energy per unit surface area of the wave is then the sum of the potential and kinetic energy. Denoting E as the total average energy per unit surface area

$$E = \overline{\mathrm{KE}} + \overline{\mathrm{PE}} = \tfrac{1}{8}\rho g H^2 \tag{4.75}$$

The total energy per wave per unit width is then simply

$$E_L = \tfrac{1}{8}\rho g H^2 L \tag{4.76}$$

It is worthwhile emphasizing that neither the average (over a wave length) potential nor kinetic energy per unit area depends on water depth or wave length, but each is simply proportional to the square of the wave height.

4.7.3 Energy Flux

Small-amplitude water waves do not transmit mass as they propagate across a fluid, as the trajectories of the water particles are closed.[4] However, water waves do transmit energy. For example, consider the waves generated by a stone impacting on an initially quiescent water surface. A portion of the kinetic energy of the stone is transformed into wave energy. As these waves travel to and perhaps break on the shoreline, it is clear that there has been a transfer of energy away from the generation area. The rate at which the energy is transferred is called the *energy flux* $\mathcal{F}$, and for linear theory it is the rate at which work is being done by the fluid on one side of a vertical section on the fluid on the other side. For the vertical section AA', shown in Figure 4.10, the instantaneous rate at which work is being done by the dynamic pressure $[p_D = (p + \rho gz)]$ per unit width in the direction of wave propagation is

$$\mathcal{F} = \int_{-h}^{\eta} p_D \cdot u\, dz \tag{4.77}$$

[4]For finite-amplitude waves, there is a mass flux; see Chapter 10.

The average energy flux is obtained as before by averaging over a wave period

$$\overline{\mathcal{F}} = \frac{1}{T}\int_t^{t+T}\int_{-h}^{\eta} p_D \cdot u \, dz \, dt \tag{4.78}$$

$$= \frac{1}{T}\int_t^{t+T}\int_{-h}^{\eta}\left[\rho g\eta \frac{\cosh k(h+z)}{\cosh kh}\right]\left[\frac{gHk}{2\sigma}\frac{\cosh k(h+z)}{\cosh kh}\cos(kx-\sigma t)\right] dz\, dt$$

from Eqs. (4.22) and (4.3b) for p and u, or

$$\overline{\mathcal{F}} = \frac{1}{T}\int_t^{t+T}\int_{-h}^{\eta}\left[\rho g\eta\frac{\cosh k(h+z)}{\cosh kh}\right]\left[\sigma\eta\frac{\cosh h(h+z)}{\sinh kh}\right] dz\, dt \tag{4.79}$$

using the dispersion relationship.

To retain terms to the second order in wave height, it is only necessary to integrate up to the mean free surface.

$$\overline{\mathcal{F}} = \frac{1}{T}\int_t^{t+T}\int_{-h}^{0}\rho g\sigma\eta^2\frac{\cosh^2 k(h+z)}{\cosh kh \sinh kh}\, dz\, dt \tag{4.80}$$

$$\overline{\mathcal{F}} = \frac{\rho g\sigma}{4k}\left(\frac{H}{2}\right)^2\frac{(2kh+\sinh 2kh)}{\sinh 2kh}$$

$$\overline{\mathcal{F}} = \left(\frac{1}{8}\rho gH^2\right)\frac{\sigma}{k}\left[\frac{1}{2}\left(1+\frac{2kh}{\sinh 2kh}\right)\right]$$

$$\overline{\mathcal{F}} = ECn \tag{4.81}$$

where Cn is the speed at which the energy is transmitted; this velocity is called the group velocity C_g, for reasons to be explained shortly.

$$C_g = nC \tag{4.82a}$$

or

$$n = \frac{C_g}{C} = \frac{1}{2}\left(1+\frac{2\,kh}{\sinh 2\,kh}\right) \tag{4.82b}$$

The factor n has as deep and shallow water asymptotes the values of $\frac{1}{2}$ and 1, respectively. Therefore, in deep water, the energy is transmitted at only half the speed of the wave profile, and in shallow water, the profile and energy travel at the same speed.

Origin of the term "group velocity." We have just derived the group velocity in terms of the rate at which energy is being transferred by a train of propagating waves. A more descriptive explanation of the term group velocity results from examining the propagation of a group of waves.

If there are two trains of waves of the same height propagating in the same direction with slightly different frequencies and wave numbers, they

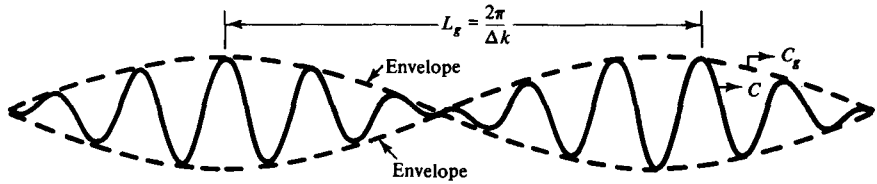

Figure 4.12 Characteristics of a "group" of waves.

are superimposed as

$$\eta = \eta_1 + \eta_2 \tag{4.83}$$

$$= \frac{H}{2}\cos(k_1 x - \sigma_1 t) + \frac{H}{2}\cos(k_2 x - \sigma_2 t) \tag{4.84}$$

where[5]

$$\sigma_1 = \sigma - \frac{\Delta\sigma}{2}, \qquad k_1 = k - \frac{\Delta k}{2}$$

$$\sigma_2 = \sigma + \frac{\Delta\sigma}{2}, \qquad k_2 = k + \frac{\Delta k}{2} \tag{4.85}$$

Using trigonometric identities, the profiles can be combined in the following manner:

$$\eta = H\cos\left[\frac{1}{2}[(k_1 + k_2)x - (\sigma_1 + \sigma_2)t]\right]\cos\left[\frac{1}{2}[(k_1 - k_2)x - (\sigma_1 - \sigma_2)t]\right]$$

$$= H\cos(kx - \sigma t)\cos\left[\frac{1}{2}\Delta k\left(x - \frac{\Delta\sigma}{\Delta k}t\right)\right] \tag{4.86}$$

The resulting profile, consisting of wave forms moving with velocity $C = \sigma/k$, is modulated by an "envelope" that propagates with speed $\Delta\sigma/\Delta k$, which is referred to as the group velocity C_g. The superimposed profile is shown in Figure 4.12. If we recall that the wave energy is proportional to the wave height, it is clear that no energy can propagate past a node as the wave height (and therefore dynamic pressure) is zero there. Therefore, the energy must travel with the speed of the *group* of waves. This velocity is seen to be, from Eq. (4.86),

$$C_g = \frac{\Delta\sigma}{\Delta k} \tag{4.87}$$

[5]This derivation is strictly true for small Δk and $\Delta\sigma$, in order that the relationships given in Eq. (4.85) satisfy the dispersion relation.

In the limit as $\Delta k \to 0$, we obtain a group velocity for a wave group of infinite length L_g (hence, a wave train of constant height), $C_g = d\sigma/dk$. This derivative can be evaluated from the dispersion relationship

$$\sigma^2 = gk \tanh kh \tag{4.88}$$

$$2\sigma \frac{d\sigma}{dk} = g \tanh kh + gkh \operatorname{sech}^2 kh$$

$$C_g = \frac{d\sigma}{dk} = \frac{(g \tanh kh + gkh \operatorname{sech}^2 kh)\sigma}{2gk \tanh kh}$$

$$= \frac{C}{2}\left(1 + \frac{2kh}{\sinh 2kh}\right) \tag{4.89}$$

Therefore, $C_g = nC$, where again

$$n = \frac{1}{2}\left(1 + \frac{2kh}{\sinh 2kh}\right) \tag{4.90}$$

4.8 TRANSFORMATION OF WAVES ENTERING SHALLOW WATER

Several changes occur as a train of waves propagates into shallow water. One of the most obvious is the change in height as the wave shoals. If energy losses (or additions) are negligible, from observation, it is evident that the waves near the point of breaking at a beach are somewhat higher than those farther offshore. Other changes, such as the previously discussed decrease in wave length with shallower depths and the changes in wave direction (Figure 4.13), are not readily apparent from the beach, but often are clearly observable from the air.

4.8.1 The Conservation of Waves Equation

In all previous derivations it has been assumed that the waves are propagating in the x direction; yet if we are discussing a coastline, it is often convenient to locate the coordinate system such that the x direction is in the onshore direction and the y direction is in the longshore direction. It is rare that waves propagate solely in the x direction once the coordinate system is prescribed.

In general, a wave crest corresponds to a line of constant wave phase. For example, if a wave train is represented as $\eta = H/2 \cos \Omega$, where Ω corresponds to the scalar phase function [recall that for waves propagating in the x direction, $\Omega = (kx - \sigma t)$]. Therefore, crests occur for $\Omega = 2n\pi$, where n is defined here as an integer. From vector analysis, the normal *unit* vector $\mathbf{n}$

Figure 4.13 Refraction of waves around a small Caribbean island. (Photo courtesy of the L.S.U. Coastal Studies Institute.)

to a scalar function is related to the normal vector **N**, which is found by taking the gradient of the function, Eq. (2.55),

$$\mathbf{N} = \nabla\Omega \tag{4.91}$$

where

$$\mathbf{N} = \mathbf{n}|\nabla\Omega| \tag{4.92}$$

and where, for purposes here, the gradient operator is only the horizontal operator

$$\nabla \equiv \nabla_h = \frac{\partial}{\partial x}\mathbf{i} + \frac{\partial}{\partial y}\mathbf{j} \tag{4.93}$$

as Ω is not a function of elevation z. The vector **N** points in the direction of the greatest change of Ω, which is the wave propagation direction.[6]

We will *define* the wave number **k** as

$$\mathbf{k} = \mathbf{n}|\nabla\Omega| = \nabla\Omega \tag{4.94}$$

[6] $\nabla\eta = (H/2)\sin\psi\nabla\psi$; thus $\nabla\eta$ is in the same direction as $\nabla\psi$. $\nabla\eta$ is the wave direction.

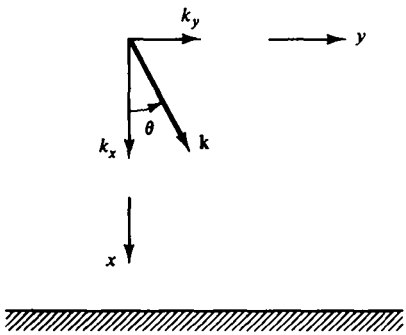

Figure 4.14 Resolution of wave number **k** into orthogonal components.

Note that for waves in the x direction that

$$\mathbf{k} = k\mathbf{i} + 0\mathbf{j} \tag{4.95a}$$

and

$$|\mathbf{k}| = k \tag{4.95b}$$

where k is the previously defined wave number. It becomes clear now that the wave number vector is nothing more than the wave number oriented in the wave direction. For waves propagating in an arbitrary direction in x-y space, we have

$$\mathbf{k} = k_x\mathbf{i} + k_y\mathbf{j} \tag{4.96}$$

and

$$|\mathbf{k}| = k = \sqrt{k_x^2 + k_y^2} \tag{4.97}$$

If an angle of incidence θ is defined as the angle made between the beach normal (the x direction) and the wave direction, then

$$\begin{aligned} k_x &= |\mathbf{k}| \cos \theta \\ k_y &= |\mathbf{k}| \sin \theta \end{aligned} \tag{4.98}$$

The phase function[7] is, therefore, $\Omega(x, y, t) = kx \cos \theta + ky \sin \theta - \sigma t = \mathbf{k} \cdot \mathbf{x} - \sigma t$. If the angle of incidence is zero, it is obvious that Ω reverts back to the simple form [Eq. (4.95a)].

The horizontal line along which waves travel is called a wave ray. It is defined (in a manner similar to a streamline) as a line along which the wave number vector is always tangent. As energy travels in the direction of the

[7]This form of the phase function can be obtained in an alternative manner. For waves of length L propagating at an angle to the x axis, the projection of the wave on the x axis has a wave length of L_x. From geometry, $L_x = L/\cos \theta$ and therefore $k_x x = (2\pi/L_x)x = k \cos \theta x$. The y contribution follows similarly.

wave, the wave energy associated with the wave travels along the wave ray also.

The angle made by the wave ray to the x axis can be obtained in the same manner as the local wave direction [see Figure 4.14]:

$$\theta = \tan^{-1} \frac{k_y}{k_x}$$

The wave frequency can be determined from the phase function as

$$\sigma = -\frac{\partial \Omega}{\partial t} \tag{4.99}$$

It is readily seen that the following expression is identically zero:

$$\frac{\partial}{\partial t}(\nabla \Omega) + \nabla\left(-\frac{\partial \Omega}{\partial t}\right) = 0 \tag{4.100}$$

which using Eqs. (4.94) and (4.99) can be written as

$$\frac{\partial \mathbf{k}}{\partial t} + \nabla \sigma = 0 \tag{4.101}$$

This equation states that any temporal variation in the wave number vector must be balanced by spatial changes in the wave angular frequency. If the wave field is constant in time, then $\nabla \sigma = 0$, or the wave period does not change with space. It is constant even as the water depth changes. If the waves encounter a steady current, it was shown in Chapter 3 that $\sigma = \mathbf{k} \cdot \mathbf{U} + \sqrt{gk \tanh kh}$, where $\mathbf{U}$ = mean current vector. Even for this case $\sigma \neq f(x, y)$, that is, only changes in $\mathbf{k}$ occur to compensate for the variable current.

To examine the conservation of waves relationship further, it is best to rederive it in a more intuitive manner. For a small length dx in the direction of wave travel, shown in Figure 4.15, we will relate the number of waves entering and leaving the block of fluid to the accumulation of waves within it. The rate at which waves enter the column is $1/T$ or $\sigma/2\pi$. The rate at which waves are leaving the column a distance dx away is found by using the first-order Taylor series. The difference in inflow and efflux of waves must be equal

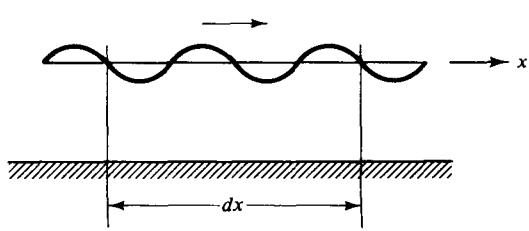

Figure 4.15 Consideration of conservation of waves.

to the accumulation of waves within the region with time, that is, the time rate of change of the number N of waves within the column,

$$\frac{\partial N}{\partial t} = \frac{\partial}{\partial t}\frac{dx}{L} = \frac{\partial}{\partial t}\left(k\frac{dx}{2\pi}\right) = \frac{dx}{2\pi}\frac{\partial k}{\partial t} \tag{4.102}$$

Equating, we have

$$\frac{\sigma}{2\pi} - \left(\frac{\sigma}{2\pi} + \frac{1}{2\pi}\frac{\partial \sigma}{\partial x}dx\right) = +\frac{dx}{2\pi}\frac{\partial k}{\partial t}$$

or

$$\frac{\partial k}{\partial t} + \frac{\partial \sigma}{\partial x} = 0 \tag{4.103}$$

which agrees with Eq. (4.101) when applied in the direction of the waves.

4.8.2 Refraction

Referring back to Eq. (4.94), the wave number vector is the gradient of a scalar. If we take the curl of $\mathbf{k}$, we find that

$$\nabla \times \mathbf{k} = 0 \tag{4.104}$$

by the identity that the curl of a gradient is zero. This irrotationality condition on $\mathbf{k}$ indicates that the line integral $\int \mathbf{k} \cdot d\mathbf{l}$ is independent of path (Chapter 2). Rewriting the integral, we have $\int \nabla\Omega \cdot d\mathbf{l} = \int d\Omega$. Therefore, the irrotationality implies that $\Omega(x, y, t)$ is uniquely determined at each point (for fixed t).

Substituting the components of $\mathbf{k}$ yields

$$\frac{\partial(k \sin\theta)}{\partial x} - \frac{\partial(k \cos\theta)}{\partial y} = 0 \tag{4.105}$$

For a shoreline where the alongshore variations in the y direction of all variables are zero, that is, there are straight and parallel offshore contours, this equation reduces to

$$\frac{d(k \sin\theta)}{dx} = 0 \tag{4.106}$$

or

$$k \sin\theta = \text{constant} \tag{4.107}$$

Therefore, the longshore projection of the wave number is a constant.

Dividing by σ in the steady-state case,

$$\frac{\sin\theta}{C} = \text{constant} \tag{4.108}$$

The constant is most readily evaluated in deep water, yielding Snell's law:

$$\boxed{\frac{\sin\theta}{C} = \frac{\sin\theta_0}{C_0}} \tag{4.109}$$

This equation, originally found in geometric optics, relates the change in direction of a wave to the change in wave celerity. Yet from before we know that waves slow down in shallower water; therefore, Snell's law indicates that for coastlines with straight and parallel contours, the wave direction θ decreases as the wave shoals, tending to make the waves approach shore normally.

In general, however, offshore contours are irregular and vary along a coast, so that the full equation must be used.

$$\frac{\partial\, k \sin\theta}{\partial x} - \frac{\partial\, k\cos\theta}{\partial y} = 0 \tag{4.110}$$

or

$$k\cos\theta\frac{\partial\theta}{\partial x} + k\sin\theta\frac{\partial\theta}{\partial y} = \cos\theta\frac{\partial k}{\partial y} - \sin\theta\frac{\partial k}{\partial x} \tag{4.111}$$

This first-order nonlinear partial differential equation for θ must be solved by computer techniques for a general coastline (see Noda *et al.*, 1974) to give the wave directions for various locations and water depths.

Historically, ray-tracing techniques were developed to solve this equation following the path of the waves. We can transform Eq. (4.111) into one valid for a coordinate system (**s**, **n**) such that **s** is in the wave direction and **n** normal to it (see Figure 4.16), defined as

$$x = \mathbf{s}\cos\theta - \mathbf{n}\sin\theta \tag{4.112a}$$

$$y = \mathbf{s}\sin\theta + \mathbf{n}\cos\theta$$

Using the chain rule the derivative operators in the **s** and **n** directions can be

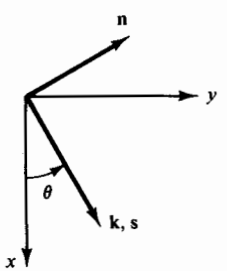

Figure 4.16 Coordinate system (**s**, **n**) defined by direction of wave number vector **k**.

established,

$$\frac{\partial}{\partial s} = \frac{dx}{ds}\frac{\partial}{\partial x} + \frac{dy}{ds}\frac{\partial}{\partial y} \tag{4.112b}$$

$$= \cos\theta \frac{\partial}{\partial x} + \sin\theta \frac{\partial}{\partial y}$$

and correspondingly,

$$\frac{\partial}{\partial n} = -\sin\theta \frac{\partial}{\partial x} + \cos\theta \frac{\partial}{\partial y} \tag{4.112c}$$

It is clear that the equation governing the wave angle can be rewritten as

$$\frac{\partial\theta}{\partial s} = \frac{1}{k}\frac{\partial k}{\partial n} = -\frac{1}{C}\frac{\partial C}{\partial n} \tag{4.113}$$

with $k = \sigma/C$. This equation relates the curvature of the wave ray to the logarithmic derivative of the wave number normal to the wave direction.

Ray tracing is often done by hand calculation,[8] as well as by computer programs. The procedure involves using Snell's law locally at each contour line of the offshore bathymetry that must be known. First a "smoothing" procedure is used to remove sharp changes of direction of the contour lines. The proper amount of smoothing is unfortunately a matter of judgment. Then the deep water wave period and angle of incidence must be known. Drawing the deep water wave crest on the bathymetry chart offshore of the $(h/L_0 = 0.5)$ contour provides the starting point for each of the rays, which are spaced at equal intervals. These intervals are chosen to give sufficient detail in the nearshore zone. For each of the contours representing a known depth, the wave celerity is determined. A ray is then drawn from the deep water crest location to the first intersection of a contour for which the wave feels bottom. At this point, a locally straight contour line is assumed and constructed by making a line segment tangent to the point of intersection. The normal to this line provides a means to calculate the angle of incidence with respect to the contour. Using Snell's law [Eq. (4.109)], the angle to which the wave is refracted is computed. The ray is then extended to the next contour and the process repeated. This can be tedious and several aids have been constructed to aid in this process (see the *Shore Protection Manual*).

4.8.3 Conservation of Energy

For conservation of energy, in a steady-state case, where there are not any energy losses or inputs, equations are developed readily relating the wave

[8]See, for example, the *Shore Protection Manual* (1977).

heights at two points of interest, especially for the case of straight and parallel bottom contours as in Figure 4.17. Recognizing that there is no energy flux across the wave rays, the energy flux $\overline{\mathcal{F}}$ across b_0 is the same as across b_1 and b_2. Due to the convergence or divergence of the wave rays, resulting from either refraction or actual physical boundaries, and due to changes in depth, the energy per unit area changes between b_1 and b_2. Assuming no wave reflection, the conservation of energy, Eq. (4.81), requires

$$(\mathrm{EnC})_1 b_1 = (\mathrm{EnC})_2 b_2 \tag{4.114}$$

or, using our definition for E as

$$E = \tfrac{1}{8}\rho g H^2 \tag{4.115}$$

we can solve for the wave height H_2:

$$H_2 = H_1 \sqrt{\frac{C_{g_1}}{C_{g_2}}} \sqrt{\frac{b_1}{b_2}} \tag{4.116}$$

If it is recognized that waves do not change period with depth (i.e., the wave period is a constant), then we have between deep and intermediate or shallow

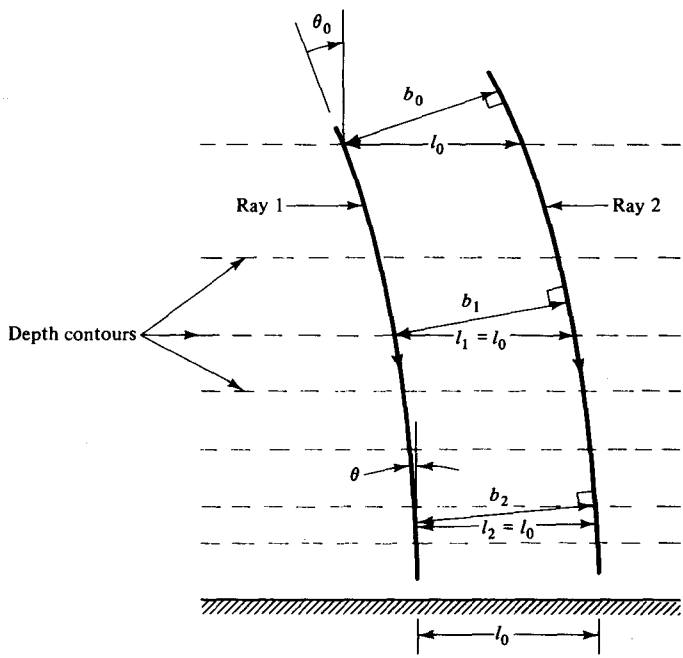

Figure 4.17 Characteristics of wave rays during refraction over idealized bathymetry.

depth water

$$H_2 = H_0\sqrt{\frac{C_0}{2C_{g_2}}}\sqrt{\frac{b_0}{b_2}} = H_0K_sK_r \tag{4.117}$$

where K_s is the shoaling coefficient and K_r the refraction coefficient. The shoaling coefficient is plotted in Figure 3.9.

In water with straight and parallel offshore contours, it is possible to determine the refraction coefficient, $(b_0/b_2)^{1/2}$, directly. In Figure 4.17 two rays are shown propagating to shore. Intuitively, since each wave refracts at the same rate along the beach, it should be expected that ray 2 is merely ray 1 displaced a constant distance l_0 in the longshore direction. This is, in fact, the interpretation of the constancy of longshore wave number given by Snell's law, $k_0 \sin \theta_0 = k \sin \theta$. From the diagram it can be seen that $b_0 = l_0 \cos \theta_0$ and

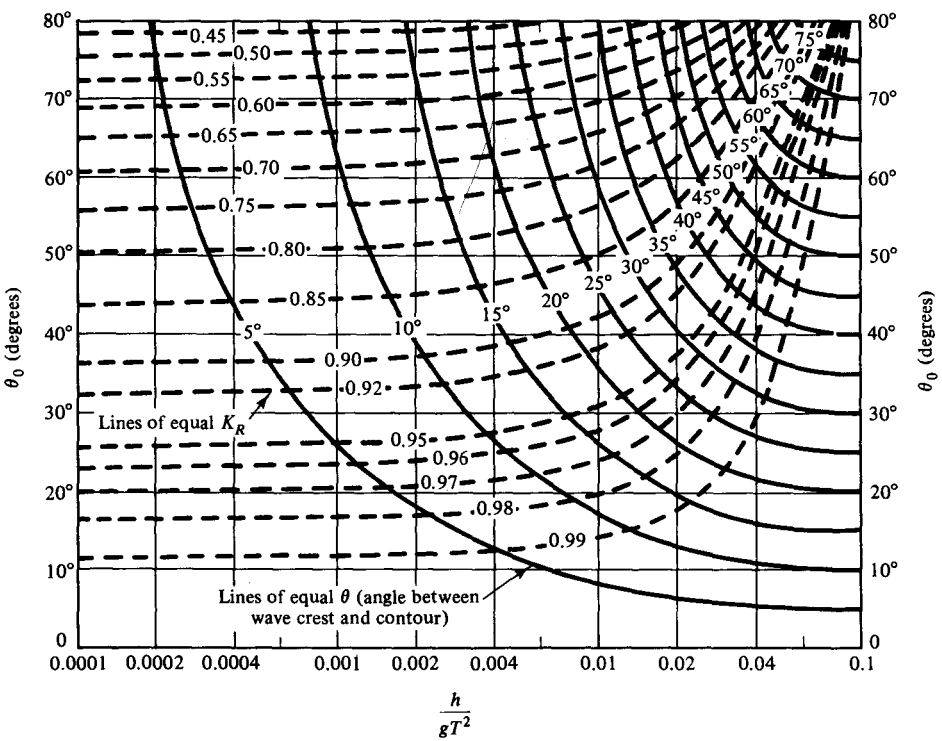

Figure 4.18 Changes in wave direction and height due to refraction on slopes with straight, parallel depth contours. (From U.S. Army Coastal Engineering Research Center, 1977.)

$b_2 = l_0 \cos \theta_2$. Therefore, the refraction coefficient K_r is

$$K_r = \left(\frac{b_0}{b_2}\right)^{1/2} = \left(\frac{\cos \theta_0}{\cos \theta_2}\right)^{1/2} = \left(\frac{1 - \sin^2 \theta_0}{1 - \sin^2 \theta_2}\right)^{1/4} \tag{4.118}$$

which is always less than unity. The perpendicular spacing between the rays always becomes greater as the wave shoals. Figure 4.18 presents a convenient means to determine K_r and wave directions from deep water characteristics. Since K_r depends on h/gT^2 and θ_0 and K_s depends only on h/gT^2, it is possible to present the product $K_r K_s$ as a function of h/gT^2 and θ_0, as shown in Figure 4.19.

Example 4.1

A wave of 2 m height in deep water approaches shore with straight and parallel contours at a 30° angle and has a wave period of 15 s. In water of 8 m, what is the direction of the wave, and what is its wave height?

Solution. Using Figure 4.18, $h/gT^2 = 0.0036$ and therefore $\theta \simeq 10.5°$ and $K_r = 0.94$. The value of K_s, using the C_g/C_0 curve of Figure 3.9, is computed to be 1.2. $H = 2(0.94)(1.2) = 2.26$ m. This result can also be obtained directly from Figure 4.19 [i.e., $K_r K_s = 1.13$ and $H = 2(1.13) = 2.26$ m].

In ray-tracing procedures, the separation distance b can be found analytically (Munk and Arthur, 1952). From Figure 4.20 it can be seen, for waves traveling with celerity C in the s direction, that the velocity components are

$$\frac{ds}{dt} = C, \qquad \frac{dx}{dt} = C \cos \theta, \qquad \frac{dy}{dt} = C \sin \theta \tag{4.119}$$

Given C and θ, these equations serve to provide the locations along the ray path.

At A, $d\theta = (\partial\theta/\partial n)b$ and, also $db = d\theta\, ds$, which is the first-order change in arc length due to the angle increment $d\theta$. Substituting for $d\theta$ in these two equations yields

$$\frac{1}{b}\frac{\partial b}{\partial s} = \frac{\partial \theta}{\partial n} \tag{4.120a}$$

or, defining $\beta = b/b_0$, where b_0 is an initial reference spacing of the wave ray, we obtain

$$\frac{1}{\beta}\frac{\partial \beta}{\partial s} = \frac{\partial \theta}{\partial n} \tag{4.120b}$$

This equation, which relates the change in spacing along the ray to the change in θ in the normal direction, is similar in form to Eq. (4.113), which also involves θ.

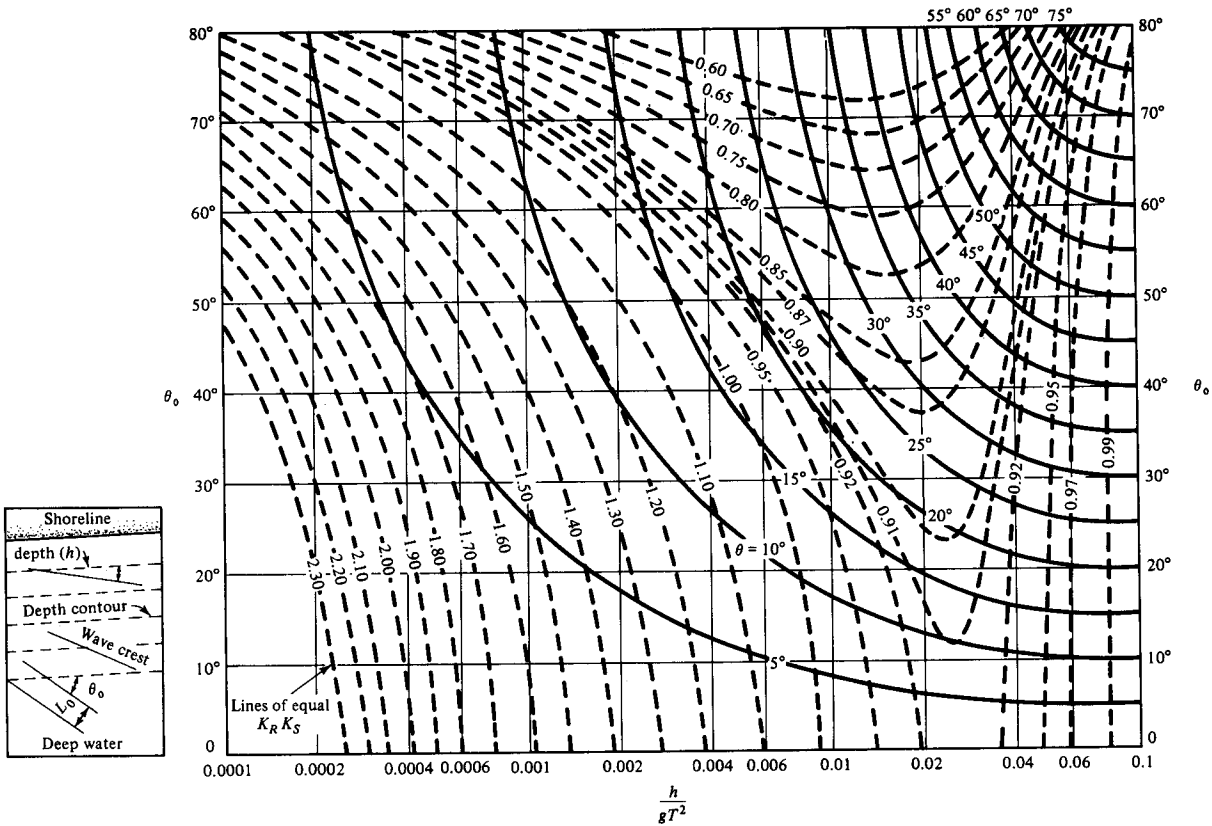

Figure 4.19 Change in wave direction and height due to refraction on slopes with straight, parallel depth contours including shoaling. (From U.S. Army Coastal Engineering Research Center, 1977.)

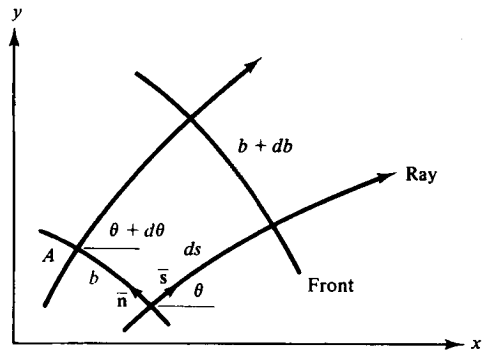

Figure 4.20 Schematic diagram showing adjacent rays.

An ordinary differential equation can be obtained for β by computing the mixed derivatives

$$\frac{\partial}{\partial n}\frac{\partial \theta}{\partial s} - \frac{\partial}{\partial s}\frac{\partial \theta}{\partial n}$$

Using the defnitions for the $\partial/\partial n$, $\partial/\partial s$ operators [Eqs. (4.112b) and (4.112c)], we obtain

$$\frac{\partial}{\partial n}\frac{\partial \theta}{\partial s} - \frac{\partial}{\partial s}\frac{\partial \theta}{\partial n} = \left(\frac{\partial \theta}{\partial x}\right)^2 + \left(\frac{\partial \theta}{\partial y}\right)^2 = \left(\frac{\partial \theta}{\partial s}\right)^2 + \left(\frac{\partial \theta}{\partial n}\right)^2$$
$$= \frac{1}{C^2}\left(\frac{\partial C}{\partial n}\right)^2 + \frac{1}{\beta^2}\left(\frac{\partial \beta}{\partial s}\right)^2$$

after substituting from Eqs. (4.113) and (4.120b). Note that the right-hand side is nonzero; this is due to the fact that the derivative operators are functions of θ.

If we cross-differentiate Eqs. (4.113) and (4.120b) directly for the mixed derivative expressions, the following results:

$$\frac{\partial}{\partial n}\frac{\partial \theta}{\partial s} - \frac{\partial}{\partial s}\frac{\partial \theta}{\partial n} = -\frac{1}{C}\frac{\partial^2 C}{\partial n^2} + \frac{1}{C^2}\left(\frac{\partial C}{\partial n}\right)^2 - \frac{1}{\beta}\frac{\partial^2 \beta}{\partial s^2} + \frac{1}{\beta^2}\left(\frac{\partial \beta}{\partial s}\right)^2$$

again, a nonzero right-hand side. If we now equate the two right-hand sides, we have

$$\frac{\partial^2 \beta}{\partial s^2} + \frac{1}{C}\frac{\partial^2 C}{\partial n^2}\beta = 0 \tag{4.121a}$$

This equation can be used to obtain β; however, it involves knowledge of the wave fronts in order to determine derivatives in the n direction. If we

evaluate the second term, we have

$$\frac{1}{C}\frac{\partial^2 C}{\partial n^2} = \frac{1}{C}\left(\sin^2\theta\frac{\partial^2 C}{\partial x^2} - 2\sin\theta\cos\theta\frac{\partial^2 C}{\partial x\,\partial y} + \cos^2\theta\frac{\partial^2 C}{\partial y^2} - \frac{\partial C}{\partial s}\frac{\partial\theta}{\partial n}\right)$$

but $\partial\theta/\partial n = (1/\beta)(\partial\beta/\partial s)$ from Eq. (4.120b).

Therefore, finally β is given by

$$\frac{d^2\beta}{ds^2} + p\frac{d\beta}{ds} + q\beta = 0 \tag{4.121b}$$

where

$$p(s) = -\frac{\cos\theta}{C}\frac{dC}{dx} - \frac{\sin\theta}{C}\frac{\partial C}{\partial y}$$

and

$$q(s) = \frac{\sin^2\theta}{C}\frac{\partial^2 C}{\partial x^2} - 2\frac{\sin\theta\cos\theta}{C}\frac{\partial^2 C}{\partial x\,\partial y} + \frac{\cos^2\theta}{C}\frac{\partial^2 C}{\partial y^2}$$

Equations (4.121b) and (4.119) provide four ordinary differential equations which can be solved simultaneously to provide locations along the ray and the spacing between the rays over a given bathymetry for which $C(x, y)$ is available (through the dispersion relationship). Numerous ray-tracing programs have been written (see, e.g., Wilson, 1966) and a recent example from Noda (1974) is presented in Figure 4.21.

Wave heights along a ray are related to β, as shown in the preceding section. Similarly to Eq. (4.117), we have

$$H = H_0\sqrt{\frac{C_0}{2C_g}}\sqrt{\frac{1}{\beta}}$$

4.8.4 Waves Breaking in Shallow Water

The shoaling coefficient indicates that the wave height will approach infinity in very shallow water, which clearly is unrealistic. At some depth, a wave of given characteristics will become unstable and break, dissipating energy in the form of turbulence and work against bottom friction. When designing a structure which at times may be inside the surf zone it becomes necessary to be able to predict the location of the breaker line.

The means by which waves break depends on the nature of the bottom and the characteristics of the wave. See Figure 4.22. For very mildly sloping beaches, typically the waves are *spilling* breakers and numerous waves occur within the surf zone (defined as that region where the waves are breaking, extending from the dry beach to the seaward limit of the breaking). *Plunging* breakers occur on steeper beaches and are characterized by the crest of the

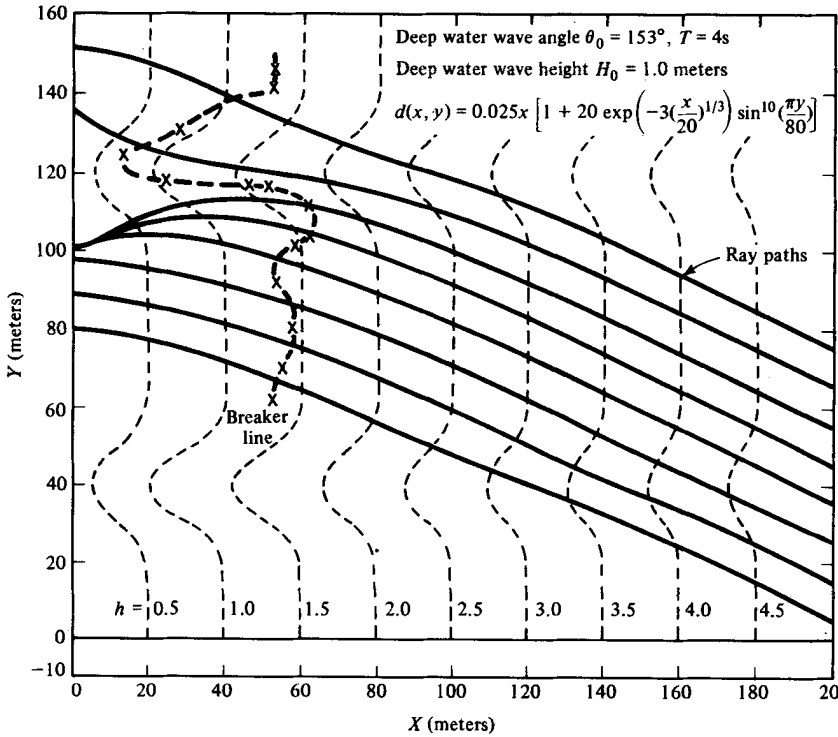

Figure 4.21 Ray lines for oblique wave incidence on a beach in the periodic rip channels. (From Noda, 1974.)

wave curling over forward and impinging onto part of the wave trough. These waves can be spectacular when air, trapped inside the "tube" formed by the wave crest, escapes by bursting through the back of the wave or by blowing out at a nonbreaking section of wave crest. *Surging* breakers occur on very steep beaches and are characterized by narrow or nonexistent surf zones and high reflection. Galvin (1968) has identified *collapsing* as a fourth classification, which is a combination of plunging and surging.

The earliest breaker criterion was that of McCowan (1894), who determined that waves break when their height becomes equal to a fraction of the water depth

$$H_b = \kappa h_b \tag{4.122a}$$

where $\kappa = 0.78$ and the subscript b denotes the value at breaking. Weggel (1972) reinterpreted many laboratory results, showing a dependency of breaker height on beach slope m. His results were

$$\kappa = b(m) - a(m)\frac{H_b}{gT^2} \tag{4.122b}$$

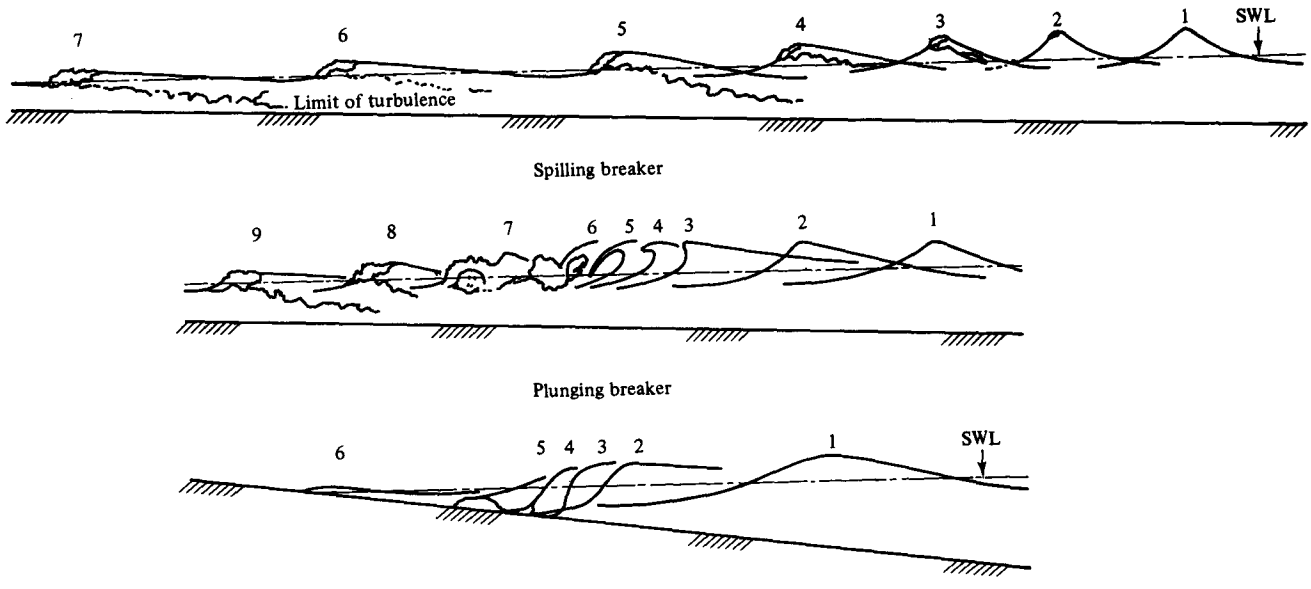

Figure 4.22 Three types of wave breaking on beaches. Small figures denote different stages of the breaking process. (Figure courtesy of I. A. Svendsen.)

where

$$a(m) = 43.8(1.0 - e^{-19m})$$

$$b(m) = 1.56(1.0 + e^{-19.5m})^{-1}$$

which approaches $\kappa = 0.78$ as the beach slope m approaches zero.[9] See Figure 12.7.

As a first approximation, the depth of wave breaking can be determined by the shoaling and refraction formulas for straight and parallel contours if the offshore wave characteristics are known.

$$H = H_0 \left(\frac{C_0}{2nC}\right)^{1/2} \left(\frac{\cos \theta_0}{\cos \theta}\right)^{1/2} \tag{4.123}$$

For shallow water, this is approximately equal to

$$H = H_0 \left(\frac{C_0}{2\sqrt{gh}}\right)^{1/2} \left(\frac{\cos \theta_0}{1}\right)^{1/2} \tag{4.124}$$

if it is assumed that the breaking angle is small. Using McCowan's breaking criterion, we have

$$\kappa h_b = H_0 \left[\frac{C_0}{2\sqrt{gh_b}} (\cos \theta_0)\right]^{1/2} \tag{4.125}$$

and solving for h_b yields

$$h_b = \frac{1}{g^{1/5}\kappa^{4/5}} \left(\frac{H_0^2 C_0 \cos \theta_0}{2}\right)^{2/5} \tag{4.126}$$

or for a plane beach where $h = mx$ and $m = \tan \beta$, the beach slope, the distance to the breaker line from shore is

$$x_b = \frac{h_b}{m} = \frac{1}{mg^{1/5}\kappa^{4/5}} \left(\frac{H_0^2 C_0 \cos \theta_0}{2}\right)^{2/5} \tag{4.127}$$

Finally, the breaking wave height is estimated to be

$$H_b = \kappa m x_b = \left(\frac{\kappa}{g}\right)^{1/5} \left(\frac{H_0^2 C_0 \cos \theta_0}{2}\right)^{2/5} \tag{4.128}$$

Komar and Gaughan (1972), using the conservation of wave energy flux in the manner of Munk (1949) for solitary waves, developed an equation similar to Eq. (4.128) for normally incident waves ($\theta = 0°$). Dalrymple et al. (1977) included the deep water wave angle as developed above. By comparing to a number of laboratory data sets, it appears that Eq. (4.128) underpredicts the breaking wave height by approximately 12% (with $\kappa = 0.8$). See Figure

[9]The $a(m)$ parameter originally defined by Weggel was dimensional and required use of the English system of units. The parameters $a(m)$ and $b(m)$ presented here are dimensionless.

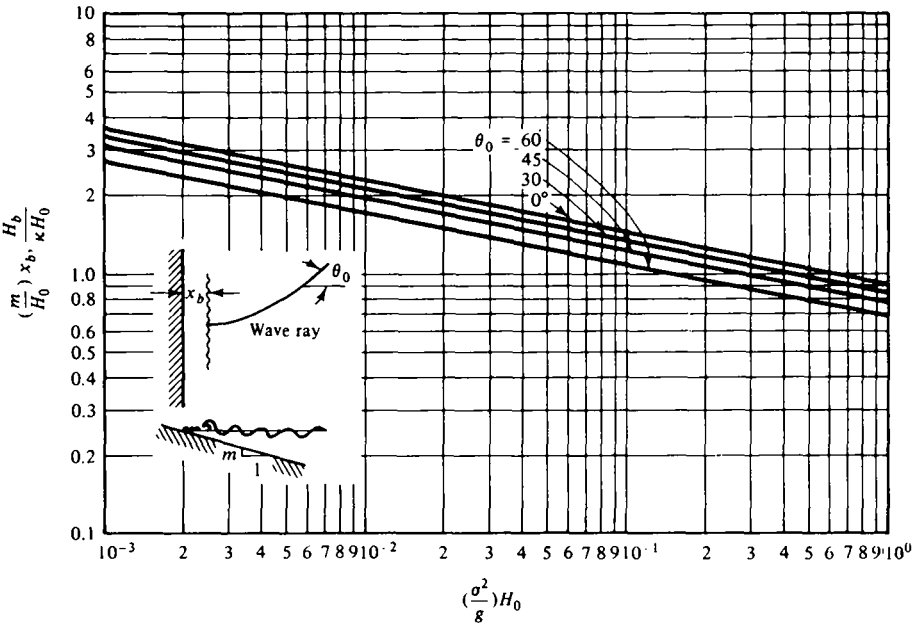

Figure 4.23 Surf zone width x_b and breaking wave height H_b versus deep water wave height H_0 in dimensionless form and as a function of θ_0, the deep water incident angle $\kappa = 0.8$.

4.23 for a dimensionless representation of Eq. (4.128). Wave breaking, with its complexities of turbulence and wave nonlinearities, is still an area of active research. The reader who must deal with design in the surf zone is referred to the literature for the most accurate prediction of surf zone width, breaking wave height, and other surf zone parameters. As an example, see Svendsen and Buhr Hansen (1976).

4.9 WAVE DIFFRACTION

Wave diffraction is the process by which energy spreads laterally perpendicular to the dominant direction of wave propagation. A simple illustration is presented in Figure 4.24, in which a wave propagates normal to a breakwater of finite length and diffraction occurs on the sheltered side of the breakwater such that a wave disturbance is transmitted into the "geometric shadow zone." It is clear that a quantitative understanding of the effects of wave diffraction is relevant to the planning and evaluation of various harbor layouts, including the extent and location of various wave-absorbing features on the perimeter. Diffraction is also important in the case of wave propagation across long distances, in which classical wave refraction effects considered alone would indicate zones of wave convergences and extremely high concentrations of wave energy. As the energy tends to be concentrated

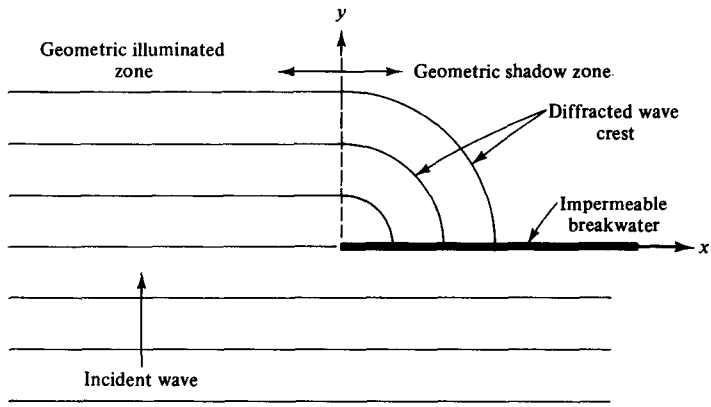

Figure 4.24 Diffraction of wave energy into geometric shadow zone behind a structure.

between a pair of converging wave orthogonals, some of this energy will "leak" across the rays toward regions of less wave energy density. Most present methodologies for computing wave energy distribution along a shoreline due to wave propagation across a shelf do not account for diffraction and may result in greatly exaggerated distributions of wave energy. In the following sections, the main contributions contained in the classical paper by Penney and Price (1952) which relate to diffraction around breakwater-like structures will be reviewed.

4.9.1 Diffraction Due to Wave–Structure Interaction

The three-dimensional linearized boundary value problem formulation for this situation is similar to that presented before [Eqs. (3.19), (3.20), (3.29), and (3.30)] for two dimensions with the exception of the no-flow condition on the structure boundary and will not be presented here. Considering water of uniform depth, the vertical dependency $Z(z)$ satisfying the no-flow bottom boundary condition is

$$Z(z) = \cosh k(h + z) \tag{4.129}$$

and the velocity potential ϕ is represented by

$$\phi(x, y, z, t) = Z(z)F(x, y)\, e^{i\sigma t} \tag{4.130}$$

where $F(x, y)$ is a complex function and $i = \sqrt{-1}$. Substituting Eq. (4.130) into the Laplace equation yields the Helmholtz equation in $F(x, y)$:

$$\frac{\partial^2 F}{\partial x^2} + \frac{\partial^2 F}{\partial y^2} + k^2 F(x, y) = 0 \tag{4.131}$$

The kinematic and dynamic free surface boundary conditions yield the usual dispersion equation

$$\sigma^2 = gk \tanh kh$$

and an equation for the water surface displacement η given by

$$\eta = \frac{i\sigma}{g} F(x, y) \cosh kh \, e^{i\sigma t} \tag{4.132}$$

The solutions to this equation will be examined for several important cases.

Normal wave incidence on a semi-infinite breakwater. An ideal (perfectly reflecting) breakwater aligned on the x axis and extending from $x = 0$ to $x = +\infty$ will require the boundary condition

$$\frac{\partial F}{\partial y} = 0, \qquad 0 < x < +\infty, \quad y = 0 \tag{4.133}$$

For the boundary condition for $x < 0$, we require that the waves be purely progressive in the positive y direction, that is,

$$F(x, y) = Ae^{-iky}, \qquad x \to -\infty, \quad \text{all } y \tag{4.134}$$

which, when combined with Eq. (4.132), yields the desired result.

The solution of the governing equations was developed by Sommerfeld (1896) and is expressed as

$$F(x, y) = \frac{1 + i}{2}\left[e^{-iky}\int_{-\infty}^{\beta} e^{-i(\pi/2)u^2}\, du + e^{iky}\int_{-\infty}^{\beta'} e^{-i(\pi/2)u^2}\, du\right] \tag{4.135}$$

where β, β', and r are defined by

$$\beta^2 = \frac{4}{L}(r - y), \qquad \beta'^2 = \frac{4}{L}(r + y), \qquad r = \sqrt{x^2 + y^2} \tag{4.136}$$

and the signs of β and β' to be taken depend on the quadrant in which the solution is being applied (see Figure 4.25). With considerable algebra, it can be verified that $F(x, y)$ as given by Eq. (4.135) satisfies both the Helmholtz equation and the boundary condition given by Eq. (4.133). The solution for $F(x, y)$ may be evaluated in terms of Fresnel integrals

$$\int_0^u \cos \tfrac{1}{2}\pi u^2\, du \qquad \text{and} \qquad \int_0^u \sin \tfrac{1}{2}\pi u^2\, du \tag{4.137}$$

which are tabluated in Abramowitz and Stegen (1965).

As $F(x, y)$ is complex, it contains both wave amplitude and phase information. As expected, at large x and $y < 0$ a standing wave is formed, at large x and y the waves approach zero, and for $x \to -\infty$, and all y, the wave is unaffected by the presence of the breakwater. Figure 4.26 represents wave

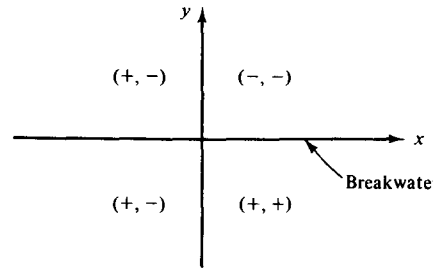

Figure 4.25 Sign criterion for (β, β').

fronts and isolines of relative wave height for $y > 0$; the horizontal scales are rendered dimensionless in terms of wave lengths.

Although the solution for $F(x, y)$ is algebraically complicated, there are several simple features that are of engineering relevance. First for large y, the relative wave height approaches one-half on a line separating the geometric shadow and illuminated regions ($x = 0$) (see Figure 4.27). Second, for $y/L > 2$, isolines of wave height behind a breakwater may be determined in

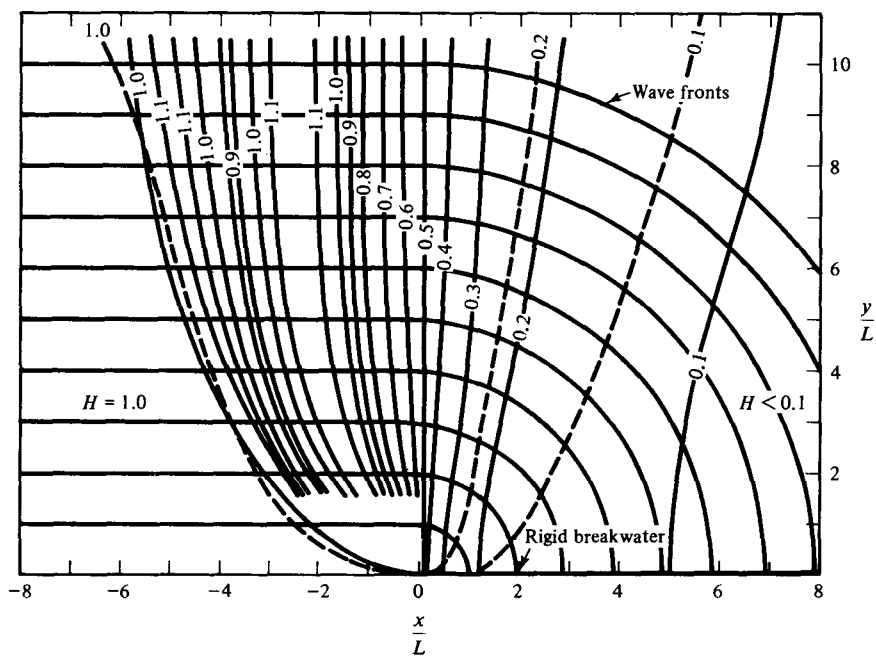

Figure 4.26 Wave fronts and contour lines of maximum wave heights in the lee of a rigid breakwater, and waves being incident normally. (————) exact solution, (- - - - -) approximate solution based on Eq. (4.138) and Figure 4.27. (After Penney and Price, 1952.)

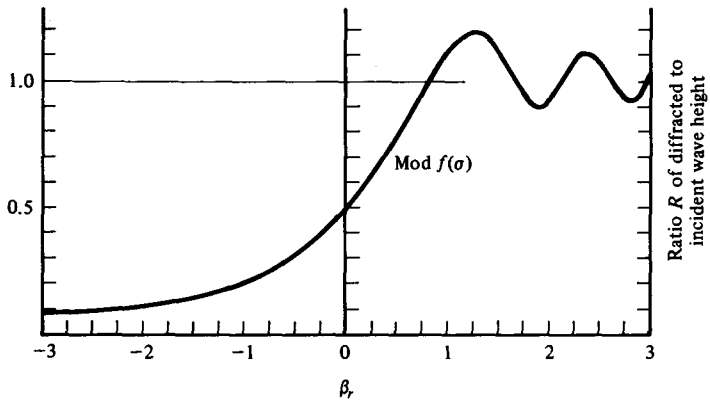

Figure 4.27 Relative diffracted wave height R versus distance parameter β_r. (From Penney and Price, 1952.)

accordance with the following parabolic equation:

$$\frac{x}{L} = \sqrt{\frac{\beta_R^4}{16} + \frac{\beta_R^2}{2}\frac{y}{L}} \tag{4.138}$$

in which β_R is the abscissa value obtained from Figure 4.27 for any value of relative wave height, $R = H/H_I$. The dashed lines in Figure 4.26 compare several isolines obtained from Eq. (4.138) and Figure 4.27 with those from the complete solution.

Obliquely incident waves on a semi-infinite breakwater. For this case, there will also be three regions or zones corresponding to (1) the geometric shadow zone, (2) the geometric illuminated zone outside the region of direct reflection from the breakwater, and (3) the up-wave region within which direct reflection from the breakwater occurs. An example of a diffraction diagram showing isolines of relative wave height is presented in Figure 4.28 for $\theta_0 = 30°$. Plots for other directions are presented in the *Shore Protection Manual* (1977). The diffracted wave fronts in the geometric shadow zone are approximated well by circles with their centers at the breakwater tip. As before, the relative wave height along a line separating the geometric sheltered and illuminated zones is approximately one-half.

Wave diffraction behind an offshore breakwater of finite length. For an offshore breakwater of finite length, an approximate diffraction diagram can be developed by considering the maximum wave height to be the sum of the two waves diffracting around each of the two ends of the breakwater. The resulting diffraction coefficients would therefore represent an upper limit, since only in very special locations would the waves reinforce completely. Figure 4.29 presents approximate isolines of diffraction coefficients for an offshore breakwater which is 10 wave lengths long.

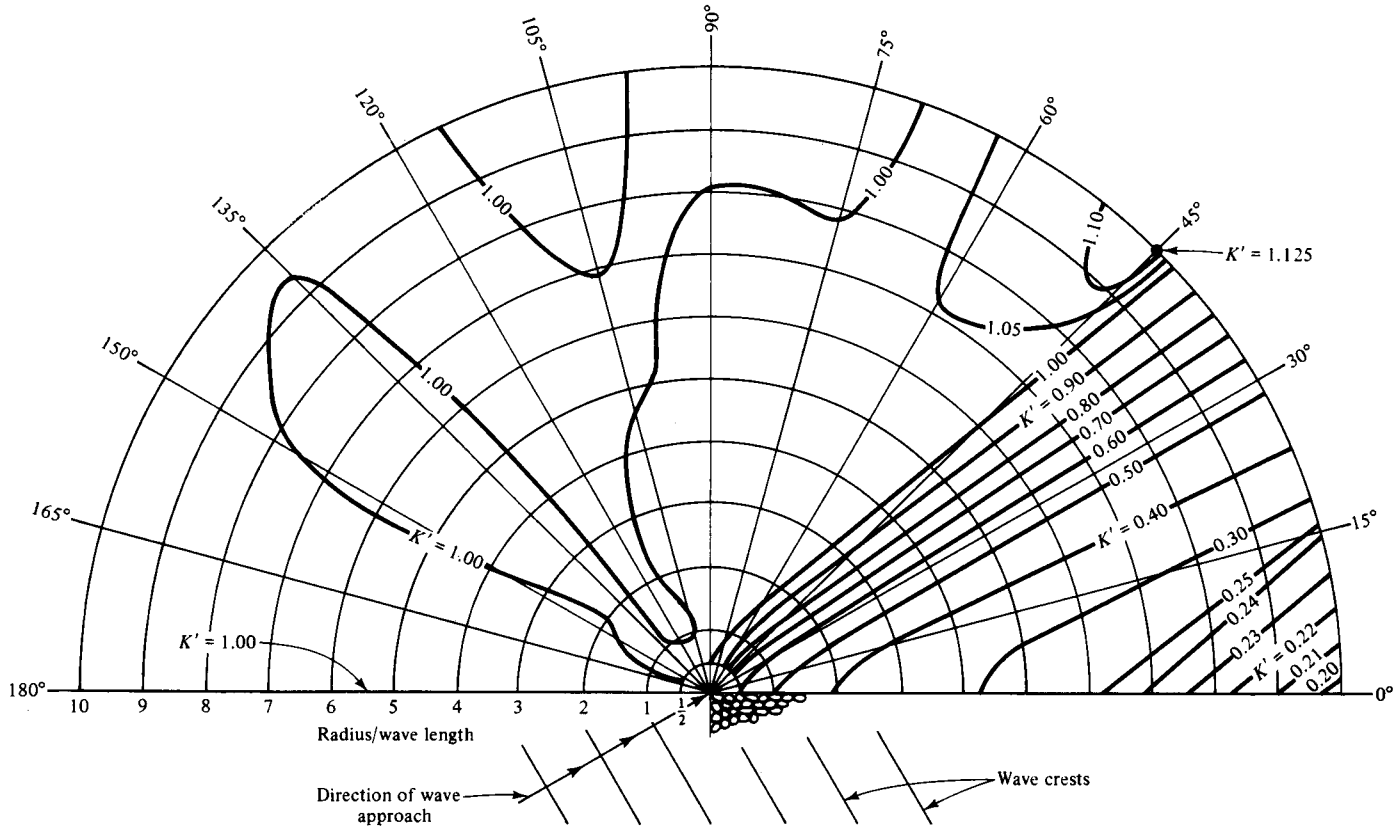

Figure 4.28 Wave diffraction by a semi-infinite impermeable breakwater, wave approach direction = 30°. (After Wiegel, 1962.)

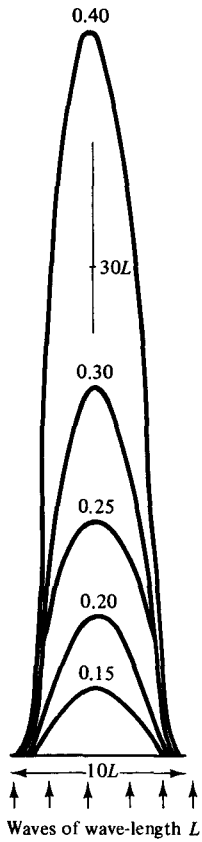

Figure 4.29 Isolines of approximate diffraction coefficients for normal wave incidence behind a breakwater that is 10 wavelengths long. (From Penney and Price, 1952.)

Wave diffraction due to waves of normal incidence propagating through a breakwater gap. For a gap width that is in excess of one wave length, it can be shown that the diffracted wave solution is very nearly given by the superposition of terms in the diffraction solution selected to approximately satisfy the boundary conditions on the two breakwater segments. Figure 4.30 presents an example for a gap that is 2.5 wave lengths long.

Waves propagating through a breakwater gap narrower than one wave length. For this case, the waves in the lee of the breakwater propagate as if from a point source and in accordance with energy conservation relationships; the wave heights decrease as $r^{-1/2}$ with distance from the center of the gap. The expression for relative wave height as a function of r for locations not too near a gap of width b is

$$\frac{H(r)}{H_0} = \frac{\pi\sqrt{b/\pi r}}{2\sqrt{kb[(\ell n\, kb/8 + \gamma)^2 + \pi^2/4]}} \tag{4.139}$$

in which γ is the Euler constant (= 0.577...).

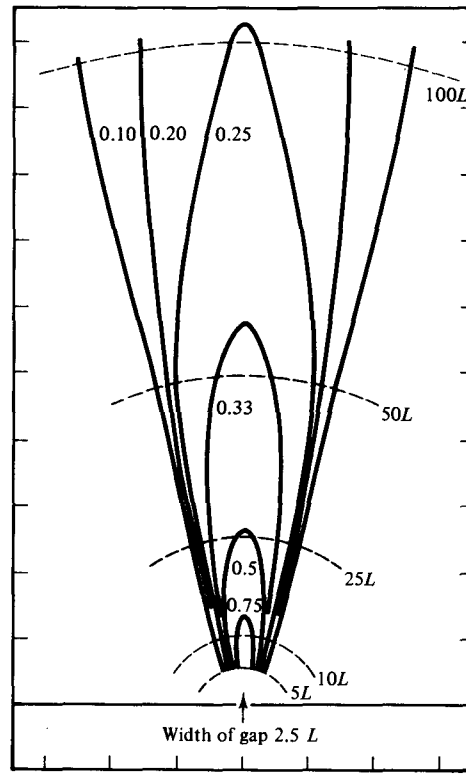

Figure 4.30 Isolines of approximate diffraction coefficients for normal wave incidence and a breakwater gap width of 2.5 wavelengths. (From Penney and Price, 1952.)

4.10 COMBINED REFRACTION–DIFFRACTION

Refraction, which involves wave direction and height changes due to depth variations, and diffraction, caused by discontinuities in the wave field resulting from the wave's interaction with structures, often occur simultaneously. For example, at the tip of a breakwater, diffraction is of utmost importance, yet if a large scour hole exists there or if a beach is nearby, refraction is important as well. It therefore is necessary to be able to treat both phenomena simultaneously.

Theoretically, the problem is difficult, demanding the solution of the Laplace equation in an irregularly varying domain. Therefore, approximations must be made to simplify the problem. The crudest approach, most often used in practice, is to assume that diffraction predominates within several wave lengths of the structure and farther away, only refraction. In the last decade, however, a newer approach has evolved through the use of a model equation. Berkhoff (1972), seeking an equation governing the propagating wave mode [which has a cosh $k(h + z)$ dependency over the depth], multiplied the Laplace equation by cosh $k(h + z)$ and integrated over the

depth. This reduces the equation to the two horizontal dimensions and yields

$$\nabla_h \cdot (CC_g \nabla_h F) + \sigma^2 \left(\frac{C_g}{C} \right) F = 0 \tag{4.140}$$

where ∇_h is the horizontal gradient operator and C and C_g are the wave and group velocity, respectively. The F is a complex function which represents the wave amplitude and phase. The total velocity potential then is

$$\phi(x, y, z) = F \cdot \frac{\cosh k(h + z)}{\cosh kh} \tag{4.141}$$

In deriving this equation it was assumed that the bottom slopes are mild. This model equation, while approximate in intermediate depth, is exact in both deep and shallow water. In deep water it reduces to Eq. (4.131), while in shallow water it is

$$g\nabla_h \cdot (h\nabla_h F) + \sigma^2 F = 0 \tag{4.142}$$

which is a two-dimensional equivalent of Eq. (5.37), valid for long waves, as discussed in Chapter 5.

Analytical solutions to the model equation are few; Jonsson and Brink-Kjaer (1973) and Smith and Sprinks (1975) present the case of waves encountering a circular island, and for Smith and Sprinks, the case for edge waves and waves propagating over a step are also treated. Kirby et al. (1981) used the model equation to study edge waves on irregular beach profiles. Numerical finite element techniques have been used by Berkhoff to treat arbitrary boundary problems such as harbors and islands.

A second approach, developed by Radder (1979) and Lozano and Liu (1980), utilizes a parabolic approximation to the elliptic Laplace equation, which makes the solution more easily obtainable as only initial condition must be specified as opposed to all the lateral boundary conditions. These methods are computationally quicker than Berkhoff's.

REFERENCES

ABRAMOWITZ, M., and I. A. STEGUN, *Handbook of Mathematical Functions*, Dover, New York, 1965.

BERKHOFF, J. C. W., "Computation of Combined Refraction–Diffraction," *Proc. 13th Conf. Coastal Eng., ASCE*, Vancouver, 1972.

DALRYMPLE, R. A., R. A. EUBANKS, and W. A. BIRKEMEIER, "Wave-Induced Circulation in Shallow Basins," *J. Waterways, Ports, Coastal Ocean Div., ASCE*, Vol. 103, Feb. 1977.

DEAN, R. G. and F. URSELL, "Interation of a Fixed Circular Cylinder with a Train of Surface Waves," MIT Hydrodynamics Laboratory Rept. T.R. No. 37, Sept. 1959.

GALVIN, C. J., "Breaker type classifications of three laboratory beaches," *J. Geophys. Res.*, Vol. 73, No. 12, 1968.

JONSSON, I. G., and O. BRINK-KJAER, "A Comparison between Two Reduced Wave Equations for Gradually Varying Depth," ISVA Prog. Rep. 31, Tech. Univ., Denmark, 1973.

KIRBY, J. T., R. A. DALRYMPLE, and P. L.-F. LIU, "Modification of Edge Waves by Barred Beach Topography," *Coastal Eng.*, Vol. 5, 1981.

KOMAR, P. D., and M. K. GAUGHAN, "Airy Wave Theory and Breaker Wave Height Prediction," *Proc. 13th Conf. Coastal Eng., ASCE*, Vancouver, 1972.

LOZANO, C. J., and P. L.-F. LIU, "Refraction–Diffraction Model for Linear Surface Water Waves," *J. Fluid Mech.*, Vol. 101, 1980.

MCCOWAN, J., "On the Highest Wave of Permanent Type," *Philos. Mag. J. Sci.*, Vol. 38, 1894.

MUNK, W. H., "The Solitary Wave Theory and Its Applications to Surf Problems," *Ann. N. Y. Acad. Sci.*, Vol. 51, 1949.

MUNK, W. H., and R. S. ARTHUR, "Wave Intensity along a Refracted Ray in Gravity Waves," Natl. Bur. Stand. Circ. 521, Washington, D. C., 1952.

NODA, E. K., "Wave-Induced Nearshore Circulation," *J. Geophys. Res.*, Vol. 79, No. 27, 1974, pp. 4097–4106.

NODA, E. K., C. J. SONU, V. C. RUPERT, and J. I. COLLINS, "Nearshore Circulation under Sea Breeze Conditions and Wave–Current Interaction in the Surf Zone," Rep. TETRA T-P-72-149-4, Tetra Tech, Inc., Pasadena, Calif., 1974.

PENNEY, W. G., and A. T. PRICE, "The Diffraction Theory of Sea Waves and the Shelter Afforded by Breakwaters," *Philos. Trans. Roy. Soc. A*, Vol. 244 (882), pp. 236–253, 1952.

RADDER, A. C., "On the Parabolic Equation Method for Water-Wave Propagation," *J. Fluid Mech.*, Vol. 95, 1979.

SMITH, R., and T. SPRINKS, "Scattering of Surface Waves by a Conical Island," *J. Fluid Mech.*, Vol. 72, 1975.

SOMMERFELD, A., "Mathematische Theorie der Diffraction," *Math. Ann.*, Vol. 47, pp. 317–374, 1896.

SVENDSEN, I. A. and J. BUHR HANSON, "Deformation Up to Breaking of Periodic Waves on a Beach," *Proc. 15th Conf. Coastal Eng., ASCE*, Honolulu, 1976.

U.S. ARMY, Coastal Engineering Research Center, *Shore Protection Manual*, Vol. I, U.S. Government Printing Office, Washington, D.C., 1977.

WEGGEL, J. R., "Maximum Breaker Height," *J. Waterways, Harbors Coastal Eng. Div., ASCE*, Vol. 98, No. WW4, Nov. 1972.

WIEGEL, R. L., "Transmission of Waves Past a Rigid Vertical Thin Barrier," *J. Waterways Harbors Div., ASCE*, Vol. 86, No. WW1, Mar. 1960.

WIEGEL, R. L., "Diffraction of Waves by a Semi-infinite Breakwater," *J. Hydraulics Div., ASCE*, Vol. 88, No. HY1, pp. 27–44, Jan. 1962.

WILSON, W. S., "A Method for Calculating and Plotting Surface Wave Rays," Tech. Memo 17, U.S. Army, Coastal Engineering Research Center, 1966.

PROBLEMS

4.1 **(a)** A wave train is propagating normally toward the coastline over bottom topography with straight and parallel contours. The deep water wave length and height are 300 m and 2 m, respectively. What are the wave length, height, and group velocity at a depth of 30 m?

(b) What is the average energy per unit surface area at the site of interest?

(c) Work part (a) for the case of the same deep water characteristics, but with deep water crests oriented at 60° to the bottom contours.

4.2 Derive the relationship for the average potential energy per unit interface area associated with the interface displacement: (*Note*: Neglect capillary effects.)

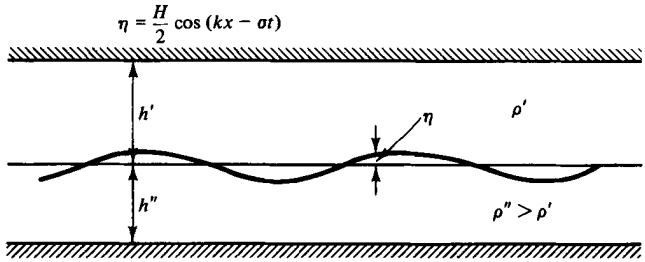

4.3 The harbor entrance shown below is designed for the following deep water wave conditions:

$$H_0 = 5 \text{ m}$$

$$T = 18 \text{ s}$$

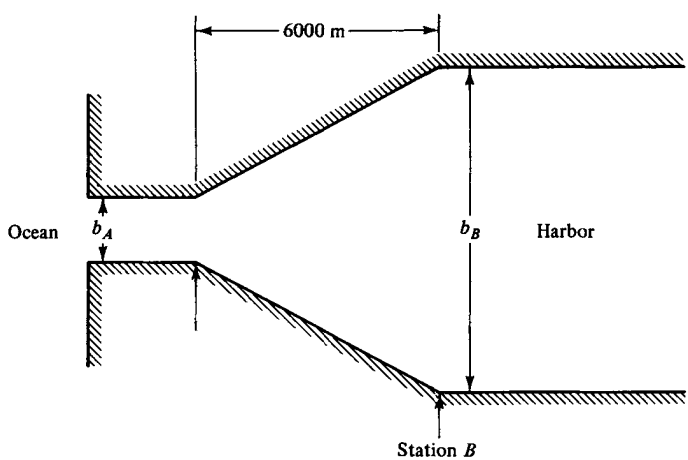

It is desired to design the width at station B such that the wave height at station B resulting from the design wave is 2 m. What must be the slope of the side

walls between A and B for this criterion to be satisfied? Use the following information:

$$b_A = 100 \text{ m}$$

$$h_A = 15 \text{ m}$$

$$h_B = 10 \text{ m}$$

and assume that the wave height is uniform across the harbor width at station B and that the spacing between orthogonals at station A is one-half that in deep water.

4.4 Observations of the water particle motions in a small-amplitude wave system have resulted in the following data for a total water depth of 1 m.

$$\text{major semiaxis} = 0.1 \text{ m}$$

$$\text{minor semiaxis} = 0.05 \text{ m}$$

These observations apply for a particle whose mean position is at middepth. What are the wave height, period, and wave length?

4.5 As a first approximation, the decrease in wave amplitude due to viscous effects can be considered to occur exponentially. For example, for a progressive wave η,

$$\eta = \frac{H_i}{2} e^{-\mu x} \cos(kx - \sigma t)$$

(a) Develop an expression corresponding to that above for the wave system resulting from a wave of height H generated at the wave maker, propagating (and suffering a loss in wave height due to viscosity) to the barrier which is at $x = \ell$, reflecting back (reflection coefficient = 1.0) and propagating back to the wavemaker. Do not consider secondary reflections from the wavemaker.

(b) Outline a laboratory procedure for determining the wave system amplitude envelope $|\eta|$.

(c) Show that

$$|\eta| = \frac{H}{2} e^{-\mu \ell} \sqrt{2\,[\cos 2k(x - \ell) + \cosh 2\mu(x - \ell)]}$$

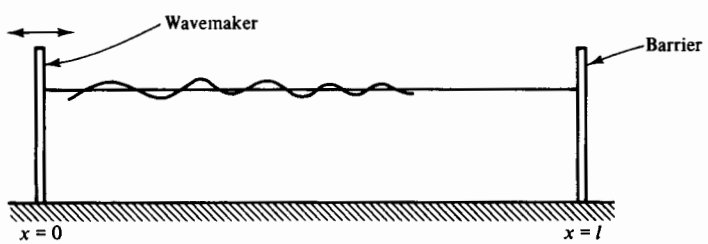

4.6 A wave of 10 s period is propagating toward the rubble mound breakwater. The recording determined by the traversing pressure sensor is shown below. Calculate the rate (per meter of width) of energy dissipation by the breakwater. At what separation distance do the pressure maxima occur?

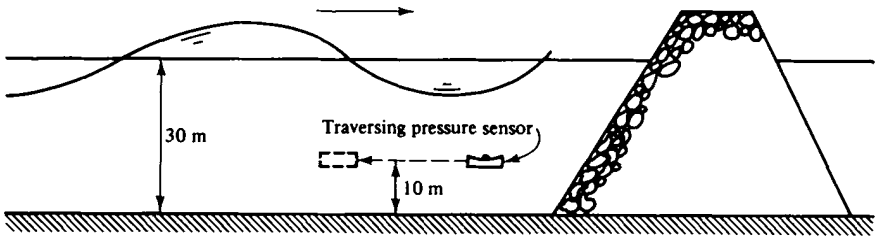

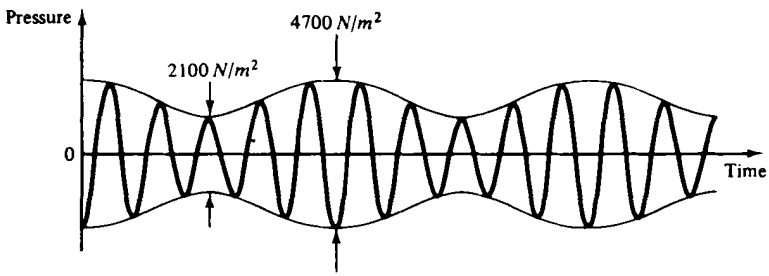

Pressure record from traversing sensor

4.7 An important problem in beach erosion control is the scour in front of vertical walls due to reflected waves. Assuming perfect reflection from a wall and shallow water conditions, determine the resulting water depth under the node nearest the wall if the wave height and period are known at the wall. Assume that the equilibrium scour depth h is one for which the maximum horizontal velocity at the bottom is less than or equal to 3 m/s.

4.8 For a group of waves in deep water, determine the time for each individual wave to pass through the group and the distance traveled by the group during that time if the spacing between the nodes of the group is L_1 and the wave period of the constituent wave is T. There are n waves in the group.

4.9 Two pressure sensors are located as shown in the sketch. For an 8-s progressive wave, the dynamic pressure amplitudes at sensors 1 and 2 are 2.07×10^4 N/m^2 and 2.56×10^4 N/m^2, respectively. What are the water depth, wave height, and wave length?

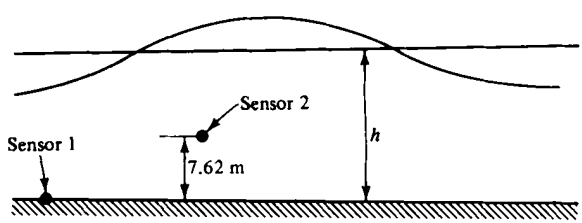

The z axis is oriented vertically upward, that is, in a direction opposed to the gravity vector. The following values may be used:

$$g = 9.81 \text{ m/s}^2$$

$$\rho = 992 \text{ kg/m}^3$$

4.10 An experiment is being conducted on the wave reflection–transmission by the step–barrier combination shown in the drawing that follows. The characteristics of the two wave envelopes are shown.

(a) What is the height Δ of the step?

(b) Is enough information given to determine whether or not energy is conserved at the step–barrier?

(c) If the answer to part (b) is "no," what additional information is required? If the answer to part (b) is "yes," determine whether energy losses occur at the step–barrier.

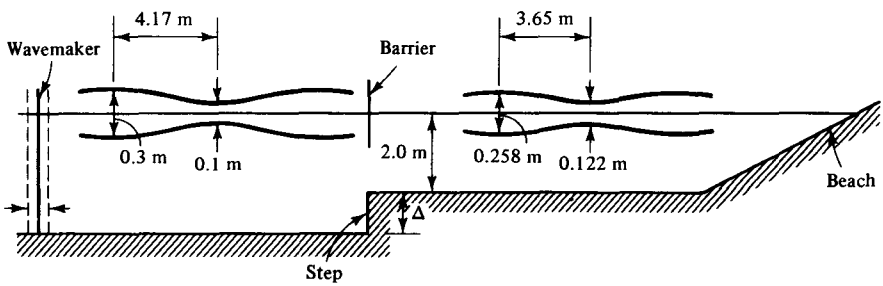

4.11 An axially symmetric wavemaker is oscillating vertically in the free surface, generating circular waves propagating radially outward. At some distance (say R_0) from the wavemaker, the crests are nearly straight over a short distance and the results derived for plane waves may be regarded as valid for the wave kinematics and dynamics at any point. The wave height at R_0 is $H(R_0)$. Derive an expression for $H(r)$, where $r > R_0$. (The depth is uniform.)

4.12 A wave with the following deep water characteristics is propagating toward the coast:

$$H_0 = 1 \text{ m}$$

$$T = 15 \text{ s}$$

At a particular nearshore site (depth = 5 m) a refraction diagram indicates that the spacing between orthogonals is one-half the deep water spacing.

(a) Find the wave height and wave length at the nearshore site.

(b) Assuming no wave refraction, but the same deep water information as in part (a), and that the wave will break when the ratio H/h reaches 0.8, in what depth does the wave break?

4.13 A wave with the following deep water characteristics is propagating toward the shore in an area where the bottom contours are all straight and parallel to the coastline:

$$H_0 = 3 \text{ m}$$

$$T = 10 \text{ s}$$

The bottom is composed of a sand of 0.1 mm diameter. If a water particle velocity of 30 cm/s is required to initiate sediment motion, what is the greatest depth in which sediment motion can occur?

4.14 For the wave system formed by the two progressive wave components

$$\eta_i = \frac{H_i}{2} \cos (kx - \sigma t + \epsilon_i)$$

$$\eta_r = \frac{H_r}{2} \cos (kx + \sigma t - \epsilon_r)$$

derive the expression for the average rate of energy propagation in the $+x$ direction.

4.15 Develop an experimental method for determining the phase shift ϵ incurred by a wave partially reflecting from a barrier.

4.16 Develop an equation for the transmitted wave height behind a vertical wall extending a depth d into the water of depth h based on the concept that the wall allows all the wave power below depth d to propagate past (Wiegel, 1960). Qualitatively, do you believe that your equation for the transmitted wave height would underestimate or overestimate the actual value? Discuss your reasons.

4.17 What is the *physical* reason that the pressure is hydrostatic under the nodes of a standing wave (to first order in wave height)?

4.18 Consider an intuitive treatment for the sum of an incident wave of height H_i and reflected wave of height H_r and show that the same envelope results are determined as obtained in the text. Represent the incident wave as two components: one of height H_r and the second as $H_i - H_r$. Now the combination of the first incident component with the reflected yields a pure standing wave and the second incident component is a pure progressive wave. Simply add the envelopes for the pure standing and progressive wave systems.

4.19 Develop the pressure response factor by integrating the linearized equation of motion from some arbitrary elevation z up to the free surface $z = \eta$.

4.20 Using as a breaking criterion that the horizontal water particle at the wave crest exceeds the wave celerity, determine breaking criteria for deep and shallow water. Why does the latter one differ from that of McCowan?